

## **Highly Porous Hydrogen-Bonded Crystals from a Triptycene-Based Catechol**

Sam Greatorex and Malcolm A. Halcrow\*

*School of Chemistry, University of Leeds, Woodhouse Lane, Leeds LS2 9JT,  
United Kingdom.*

*E-mail: m.a.halcrow@leeds.ac.uk*

**Supporting Information**

	Page
<b>Experimental Details</b>	2
<b>Table S1</b> Experimental data for the crystal structure determinations in this work.	3
<b>Table S2</b> Hydrogen bond parameters for the crystal structures of <b>1</b> .	4
<b>Fig. S1</b> View of the unique molecules in the crystal structure of <b>1</b> ·2Et <sub>2</sub> O.	5
<b>Fig. S2</b> Packing diagrams of <b>1</b> ·2Et <sub>2</sub> O.	6
<b>Fig. S3</b> The hydrogen bonding connectivity in <b>1</b> ·2Et <sub>2</sub> O, which forms a CsCl ( <b>bcu</b> ) topology net.	7
<b>Fig. S4</b> View of the asymmetric unit in the crystal structure of <b>1</b> ·3.4thf.	8
<b>Fig. S5</b> Packing diagram of <b>1</b> ·3.4thf, showing each molecule of <b>1</b> hydrogen bonding to six nearest neighbours.	9
<b>Fig. S6</b> The hydrogen bonding connectivity in <b>1</b> ·3.4thf, which forms a 4 <sup>9</sup> .6 <sup>6</sup> ( <b>acs</b> ) topology net.	10
<b>Fig. S7</b> View of the asymmetric unit in the crystal structure of <b>1</b> ·2.15CHCl <sub>3</sub> .	11
<b>Fig. S8</b> Packing diagram of <b>1</b> ·2.15CHCl <sub>3</sub> , showing each molecule of <b>1</b> hydrogen bonding to seven nearest neighbours.	12
<b>Fig. S9</b> The seven-connected hydrogen bonded net connectivity in <b>1</b> ·2.15CHCl <sub>3</sub> .	13
<b>Fig. S10</b> Views of the seven-connected hydrogen bonded net in <b>1</b> ·2.15CHCl <sub>3</sub> , emphasising its relationship to stacks of puckered 4 <sup>4</sup> sheets linked by addition pillaring connections.	14
<b>Fig. S11</b> View of the asymmetric unit in the crystal structure of <b>1</b> ·EtOAc.	15
<b>Fig. S12</b> Packing diagram of <b>1</b> ·EtOAc, showing each molecule of <b>1</b> connecting to six nearest neighbours by hydrogen bonding.	16
<b>Fig. S13</b> Packing diagrams of <b>1</b> ·EtOAc.	17
<b>Fig. S14</b> The hydrogen bonded net connectivity in <b>1</b> ·EtOAc, which forms a 4 <sup>8</sup> .5 <sup>4</sup> .6 <sup>3</sup> ( <b>bsn</b> ) net if all the connections are considered equally.	18
<b>Fig. S15</b> X-ray powder diffraction data from <b>1</b> ·2Et <sub>2</sub> O.	19
<b>Fig. S16</b> X-ray powder diffraction data from <b>1</b> ·3.4thf.	19
<b>Fig. S17</b> X-ray powder diffraction data from <b>1</b> ·2.15CHCl <sub>3</sub> .	20
<b>Fig. S18</b> X-ray powder diffraction data from a sample of <b>1</b> crystallized from ethyl acetate/pentane.	20
<b>Table S3</b> Hydrogen bond parameters for the crystal structures of <b>2</b> .	21
<b>Fig. S19</b> View of the asymmetric unit in the crystal structure of <b>2</b> ·½Et <sub>2</sub> O·½H <sub>2</sub> O.	22
<b>Fig. S20</b> Packing diagram of <b>2</b> ·½Et <sub>2</sub> O·½H <sub>2</sub> O, showing the hydrogen bonding interactions.	23
<b>Fig. S21</b> View of the 2D bilayer hydrogen bonded net in <b>2</b> ·½Et <sub>2</sub> O·½H <sub>2</sub> O.	24
<b>Fig. S22</b> Alternative view of the 2D bilayer hydrogen bonded net in <b>2</b> ·½Et <sub>2</sub> O·½H <sub>2</sub> O.	25
<b>Fig. S23</b> View of the asymmetric unit in the crystal structure of <b>2</b> ·dioxane.	26
<b>Fig. S24</b> Packing diagram of <b>2</b> ·dioxane, showing each molecule of <b>2</b> connecting to six nearest neighbours	27
<b>Fig. S25</b> The six-connected hydrogen bonded net in <b>2</b> ·dioxane.	28
<b>Fig. S26</b> View of the molecule in the crystal structure of <b>3</b> .	29
<b>Fig. S27</b> Packing diagrams of <b>3</b> .	30
<b>References</b>	31

## Experimental Details

Single crystals of **1**·2Et<sub>2</sub>O and **2**·½Et<sub>2</sub>O·½H<sub>2</sub>O were obtained by slow diffusion of diethyl ether vapour into ethanol solutions of **1** or **2**. Crystals of **1**·3.4thf, **1**·2.15CHCl<sub>3</sub>, **1**·EtOAc and **2**·dioxane were obtained similarly from solutions of **1** or **2** in those solvents, but using pentane vapour as antisolvent. Crystals of **3** formed upon standing inside an NMR tube of that compound in CDCl<sub>3</sub>. Single crystal diffraction data were measured with an Agilent Supernova dual-source diffractometer, using monochromated Mo-*K*<sub>α</sub> ( $\lambda = 0.7107 \text{ \AA}$ ) or Cu-*K*<sub>α</sub> ( $\lambda = 1.5418 \text{ \AA}$ ) radiation. The diffractometer is fitted with an Oxford Cryostream low-temperature device. Experimental data from the structure determinations are given in Table S1. The structures were all solved by direct methods (*SHELXS97*<sup>[1]</sup>), and developed by full least-squares refinement on *F*<sup>2</sup> (*SHELXL97*<sup>[1]</sup>). Crystallographic figures were prepared using *XSEED*,<sup>[2]</sup> which incorporates *POVRAY*.<sup>[3]</sup> X-ray powder diffraction patterns were measured at room temperature using a Bruker D2 Phaser diffractometer, with Cu-*K*<sub>α</sub> radiation.

Unless otherwise stated, all non-H atoms in the structure refinements were refined anisotropically, and C-bound H atoms were placed in calculated positions and refined using a riding model. Hydroxyl H atoms were located in the Fourier map, and allowed to refine subject to the fixed restraint O–H = 0.90(2) Å and with isotropic displacement parameters constrained to be 1.5x *U*<sub>eq</sub> for the corresponding O atom. Friedel opposite reflections for the structures in chiral or handed space groups were merged in the final least squares cycles, since the absolute structures of these light-atom crystals could not be determined.

The asymmetric unit of **1**·2Et<sub>2</sub>O<sup>[4]</sup> contains half a molecule of **1** spanning the crystallographic *C*<sub>2</sub> axis ½, 0, *z*, and a molecule of diethyl ether on a general crystallographic position. The solvent molecule was refined over two disorder sites with a refined occupancy ratio of 0.56:0.44. The fixed restraints C–C = 1.54(2), C–O = 1.43(2), 1,3-C...C = 2.34(2) and 1,3-C...O = 2.42(2) Å were applied to the disordered solvent. All crystallographically ordered non-H atoms were refined anisotropically.

The triptycene molecules in **1**·3.4thf pack into hydrogen bonded channels parallel to [001]. The volume of the channels is 3089 Å<sup>3</sup> per unit cell, or 59.6 % of the cell volume. Three thf molecules are resolved beside the walls of the channels, but this still leaves significant void space at their centre. A *SQUEEZE* analysis<sup>[5]</sup> identified 749 Å<sup>3</sup> of unallocated void volume per unit cell, containing 100 electrons. This is equivalent to an extra 2.5 thf molecules (100 electrons) per unit cell, or 0.4 equiv thf per formula unit. This is the formula that was used for the density and *F*(000) calculations. The *SQUEEZED* dataset was used in the final least squares cycles. All H atoms in this structure, including the hydroxyl groups, were placed in calculated positions and refined using a riding model.

The dataset of **1**·2.15CHCl<sub>3</sub> is only 84 % complete to  $2\theta = 144^\circ$  on Cu-*K*<sub>α</sub>, with weaker diffraction at higher angles that may reflect its porous structure. There are two types of channel in this crystal: small channels containing well defined chloroform molecules; and larger channels of diffuse electron density that was treated using *SQUEEZE*.<sup>[5]</sup> There are four small channels and two large ones in each unit cell. The *SQUEEZE* analysis identified 532 unresolved electrons per unit cell in the large channels, corresponding to 66.5 electrons per formula unit or 1.15 equiv chloroform (58 electrons per molecule). That is the formula used for the density and *F*(000) calculations. The total volume per unit cell of the small and large channels is 1029 and 1809 Å<sup>3</sup>, respectively, which is equivalent to 49.7 % of the unit cell volume. The well-defined chloroform molecule is disordered over two half-occupied sites that share two common Cl atoms, which was modelled without restraints. All H atoms in this structure, including the hydroxyl groups, were placed in calculated positions and refined using a riding model.

Hydroxyl group O(16) in **1**·EtOAc is disordered over two equally occupied sites, reflecting a disordered hydrogen bond between this group and its symmetry equivalent related by  $-x, -y, 2-z$ . The O atom disorder was modelled without restraints, but a distance restraint O–H = 0.90(2) Å was required to refine the hydroxyl H atoms in appropriate positions.

The asymmetric unit of **2**·½Et<sub>2</sub>O·½H<sub>2</sub>O<sup>[4]</sup> contains two molecules of **2**, one disordered molecule of diethyl ether and a disordered water molecule. The diethyl ether molecule was modelled over three sites with occupancies of 0.67, 0.20 and 0.13 using the same restraints as in **1**·2Et<sub>2</sub>O. Two Fourier peaks that were 1.0 Å apart, but not bonded to any other atom, were included in the model as a water molecule that is disordered over two sites with refined occupancies of 0.58:0.42. These water sites accept two intermolecular O–H...O hydrogen bonds, and are within hydrogen bonding distance of two other O atom acceptors. All fully occupied non-H atoms, plus the major water site, were refined anisotropically. The disordered water H atoms were not included in the model, but are accounted for in the density calculation.

No disorder is present in **2**·C<sub>4</sub>H<sub>8</sub>O<sub>2</sub> or **3**, and no restraints were applied to either refinement.

**Table S1** Experimental data for the crystal structure determinations in this work. Flack parameters for the handed structures are not included, because they could not be determined meaningfully for these light-atom crystals.

	<b>1·2Et<sub>2</sub>O<sup>a</sup></b>	<b>1·3.4thf</b>	<b>1·2.15CHCl<sub>3</sub></b>	<b>1·EtOAc</b>	<b>2·½Et<sub>2</sub>O·½H<sub>2</sub>O<sup>a</sup></b>	<b>2·C<sub>4</sub>H<sub>8</sub>O<sub>2</sub></b>	<b>3</b>
Molecular formula	C <sub>30</sub> H <sub>38</sub> O <sub>8</sub>	C <sub>35.60</sub> H <sub>45.20</sub> O <sub>9.40</sub>	C <sub>24.15</sub> H <sub>20.15</sub> Cl <sub>6.44</sub> O <sub>6</sub>	C <sub>26</sub> H <sub>26</sub> O <sub>8</sub>	C <sub>24</sub> H <sub>23</sub> O <sub>5</sub>	C <sub>26</sub> H <sub>26</sub> O <sub>6</sub>	C <sub>26</sub> H <sub>26</sub> O <sub>4</sub>
<i>M<sub>r</sub></i>	526.60	623.52	634.65	466.47	391.42	434.47	402.47
Crystal class	tetragonal	trigonal	monoclinic	triclinic	monoclinic	orthorhombic	orthorhombic
Space group	<i>I4<sub>1</sub>cd</i>	<i>P3c1</i>	<i>C2/c</i>	<i>P1̄</i>	<i>P2<sub>1</sub>/c</i>	<i>P2<sub>1</sub>2<sub>1</sub>2<sub>1</sub></i>	<i>P2<sub>1</sub>2<sub>1</sub>2<sub>1</sub></i>
<i>a</i> (Å)	13.3213(2)	23.519(4)	23.2178(16)	8.8058(5)	13.1161(4)	9.6831(2)	8.7138(4)
<i>b</i> (Å)	–	–	25.566(2)	9.1775(6)	11.8371(3)	11.9425(2)	14.7312(7)
<i>c</i> (Å)	31.0721(6)	10.8159(13)	10.7276(7)	14.0128(8)	24.8580(7)	18.3518(4)	15.9961(8)
<i>α</i> (°)	–	–	–	84.071(5)	–	–	–
<i>β</i> (°)	–	–	116.349(6)	85.136(4)	97.306(3)	–	–
<i>γ</i> (°)	–	–	–	82.927(5)	–	–	–
<i>V</i> (Å <sup>3</sup> )	5513.96(16)	5181.2(14)	5706.2(7)	1114.83(12)	3828.03(19)	2122.21(7)	2053.34(17)
<i>Z</i>	8	6	8	2	8	4	4
<i>T</i> (K)	120	120	120	120	120	120	120
<i>μ</i> (mm <sup>-1</sup> )	0.748 <sup>b</sup>	0.086 <sup>c</sup>	6.196 <sup>b</sup>	0.859 <sup>b</sup>	0.772 <sup>b</sup>	0.788 <sup>b</sup>	0.087 <sup>c</sup>
Measured reflections	4812	22120	8045	8449	15514	5791	8409
Independent reflections	1377	4455	4795	4205	7501	2372	2854
<i>R<sub>int</sub></i>	0.044	0.082	0.043	0.057	0.054	0.043	0.053
<i>R<sub>1</sub>, I &gt; 2σ(I)</i> <sup>d</sup>	0.045	0.099	0.087	0.062	0.068	0.038	0.053
<i>wR<sub>2</sub>, all data</i> <sup>e</sup>	0.120	0.272	0.284	0.194	0.206	0.099	0.125
Goodness of fit	1.072	1.102	1.046	1.042	1.036	1.055	1.064

<sup>a</sup>See also ref. [4]. <sup>b</sup>Collected with Cu-*K<sub>α</sub>* radiation. <sup>c</sup>Collected with Mo-*K<sub>α</sub>* radiation. <sup>d</sup> $R = \Sigma[|F_o| - |F_c|] / \Sigma|F_o|$ . <sup>e</sup> $wR = [\Sigma w(F_o^2 - F_c^2) / \Sigma wF_o^4]^{1/2}$ .

**Table S2** Hydrogen bond parameters for the crystal structures of **1** (Å, °).<sup>a</sup> See Figs. S1, S4, S7 and S11 for the atom numbering scheme for each structure.

	D–H	H...A	D...A	D–H...A
<b>1·2Et<sub>2</sub>O<sup>[4]</sup></b>				
O(7)–H(7)...O(17A)/O(17B)	0.889(19)	1.83(2)/1.84(2)	2.704(5)/2.699(6)	169(4)/162(4)
O(8)–H(8)...O(12 <sup>ii</sup> )	0.903(19)	1.91(2)	2.790(2)	164(4)
O(12)–H(12)...O(7 <sup>iv</sup> )	0.874(19)	1.82(2)	2.673(2)	166(3)
<b>1·3.4thf</b>				
O(7)–H(7)...O(29)	0.84	1.87	2.633(5)	149.7
O(7)–H(7)...O(8)	0.84	2.27	2.705(4)	112.9
O(8)–H(8)...O(7 <sup>x</sup> )	0.84	1.91	2.716(4)	159.5
O(15)–H(15)...O(16 <sup>xii</sup> )	0.84	1.88	2.713(7)	174.5
O(16)–H(16)...O(15)	0.84	2.28	2.711(7)	112.3
O(16)–H(16)...O(34)	0.84	1.84	2.576(8)	145.3
O(23)–H(23)...O(24 <sup>xiv</sup> )	0.84	1.88	2.722(5)	178.5
O(24)–H(24)...O(23)	0.84	2.29	2.698(5)	110.2
O(24)–H(24)...O(39)	0.84	1.83	2.597(7)	150.2
<b>1·2.15CHCl<sub>3</sub></b>				
O(7)–H(7)...O(8)	0.84	2.36	2.694(4)	104.0
O(7)–H(7)...O(8 <sup>xvi</sup> )	0.84	2.01	2.767(4)	149.2
O(8)–H(8)...O(7 <sup>xvii</sup> )	0.84	1.86	2.693(4)	168.8
O(15)–H(15)...O(23 <sup>xx</sup> )	0.84	1.89	2.717(4)	169.0
O(16)–H(16)...O(15)	0.84	2.28	2.699(4)	111.1
O(16)–H(16)...O(24 <sup>xix</sup> )	0.84	2.05	2.788(4)	145.9
O(23)–H(23)...O(24)	0.84	2.28	2.680(4)	109.9
O(23)–H(23)...O(15 <sup>xxii</sup> )	0.84	2.14	2.840(4)	141.0
O(24)–H(24)...O(16 <sup>xxi</sup> )	0.84	1.88	2.691(3)	161.5
<b>1·EtOAc</b>				
O(7)–H(7)...O(31)	0.889(18)	1.804(19)	2.687(3)	171(3)
O(8)–H(8)...O(7)	0.859(18)	2.26(3)	2.738(2)	115(3)
O(8)–H(8)...O(7 <sup>xxiii</sup> )	0.859(18)	1.99(3)	2.672(2)	136(3)
O(15)–H(15)...O(23 <sup>xvi</sup> )	0.891(18)	1.90(2)	2.776(2)	169(3)
O(16A)–H(16A)...O(31 <sup>xxv</sup> )	0.89(2)	2.03(2)	2.918(11)	179(7)
O(16B)–H(16B)...O(15)	0.89(2)	2.49(8)	2.849(9)	104(6)
O(16B)–H(16B)...O(16A <sup>xxvi</sup> )	0.89(2)	1.94(3)	2.802(6)	164(8)
O(23)–H(23)...O(24)	0.889(18)	2.09(3)	2.673(2)	123(3)
O(24)–H(24)...O(8 <sup>xxvii</sup> )	0.883(17)	1.859(18)	2.736(2)	172(3)

<sup>a</sup>Symmetry codes: (ii)  $y, 1/2-x, 1/4+z$ ; (iv)  $1-y, 1/2-x, -1/4+z$ ; (x)  $1-x, 1-y, -1/2+z$ ; (xii)  $x, x-y, 1/2+z$ ; (xiv)  $-x+y, y, 1/2+z$ ; (xvi)  $1-x, 1-y, 2-z$ ; (xvii)  $x, 1-y, 1/2+z$ ; (xix)  $-1/2+x, 1/2-y, -1/2+z$ ; (xx)  $1/2-x, 1/2-y, 1-z$ ; (xxi)  $1/2-x, 1/2-y, 2-z$ ; (xxii)  $1/2+x, 1/2-y, 1/2+z$ ; (xxiii)  $-x, 2-y, 1-z$ ; (xxv)  $x, -1+y, z$ ; (xxvi)  $-x, -y, 2-z$ ; (xxvii)  $1-x, 1-y, 1-z$ .

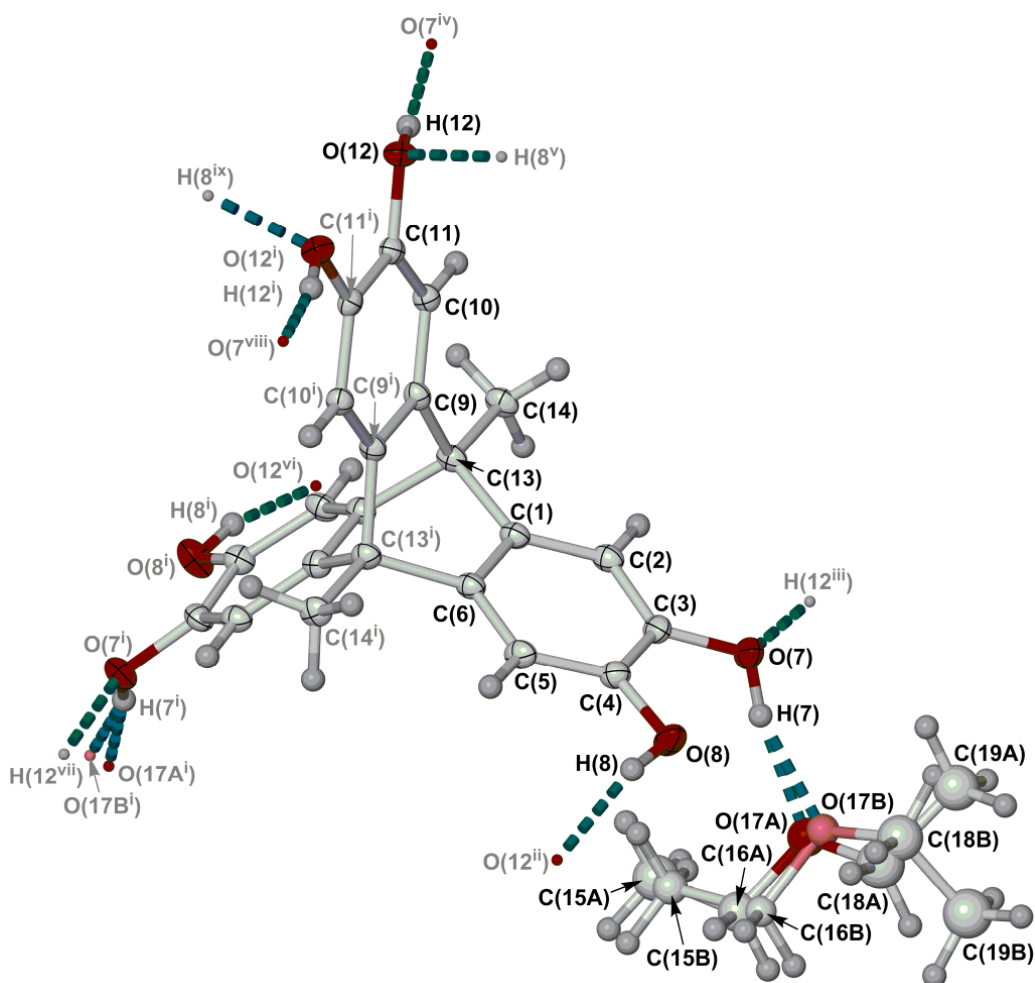


**Fig. S1.** View of the unique molecules in the crystal structure of  $1 \cdot 2\text{Et}_2\text{O}$ .<sup>[4]</sup> The molecule of **1** spans a crystallographic  $C_2$  axis, which bisects the midpoints of the C(9)–C(9<sup>i</sup>) and C(11)–C(11<sup>i</sup>) bonds.

Displacement ellipsoids are at the 50 % probability level, except for H atoms which have arbitrary radii. Both orientations of the disordered diethyl ether molecule are shown, with the 'B' orientation of the acceptor atom O(17) having paler colouration for clarity.

Colour code: C, white; H, pale grey; O, red. Symmetry codes: (i)  $1-x, -y, z$ ; (ii)  $y, 1/2-x, 1/4+z$ ; (iii)  $1/2-y, 1-x, 1/4+z$ ; (iv)  $1-y, 1/2-x, -1/4+z$ ; (v)  $1/2-y, x, -1/4+z$ ; (vi)  $1-y, -1/2+x, 1/4+z$ ; (vii)  $1/2+y, -1+x, 1/4+z$ ; (viii)  $y, -1/2+x, -1/4+z$ ; (ix)  $1/2+y, -x, -1/4+z$ .

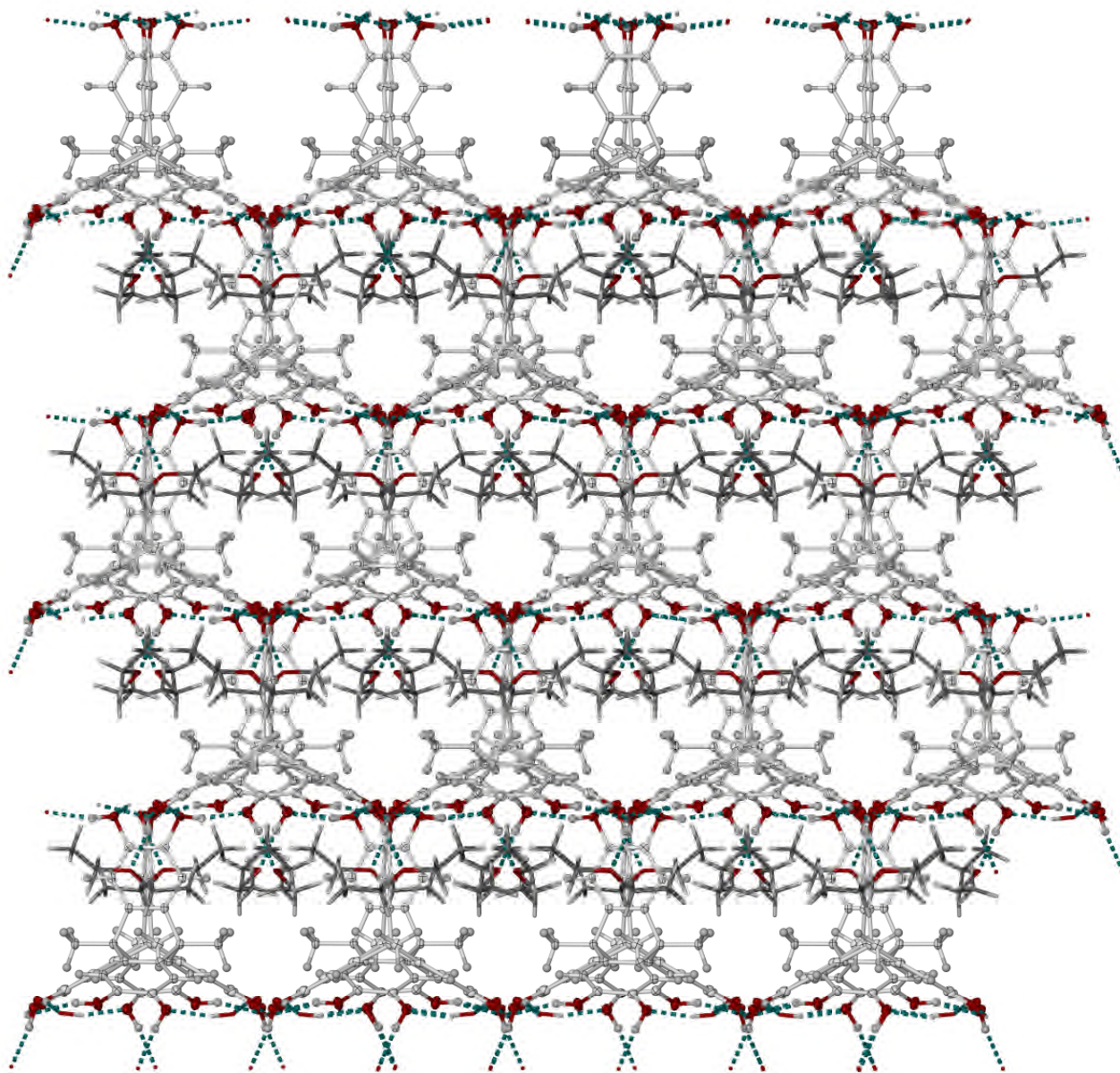


**Fig. S2.** Packing diagrams of  $1 \cdot 2\text{Et}_2\text{O}$ .<sup>[4]</sup> The view is parallel to the (110) crystal vector, with the *c* axis vertical (the same as in Fig. 2 of the main article). Only one disorder orientation of the diethyl ether molecules is shown, which are drawn with arbitrary atomic radii for clarity. Other atoms are drawn with 50 % displacement ellipsoids.

Colour code: C (**1**), white; C (solvent), dark grey; H, pale grey; O, red.



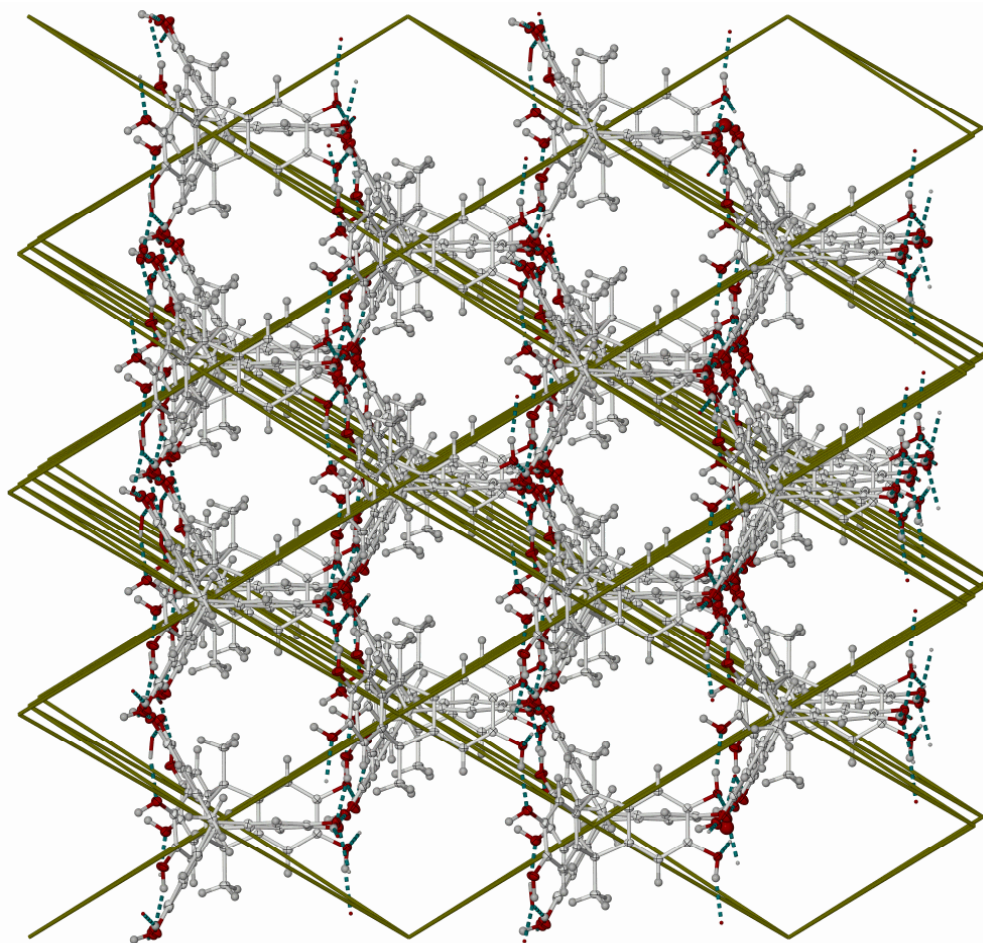


**Fig. S3.** Figure showing the hydrogen bonding connectivity in  $\mathbf{1} \cdot 2\text{Et}_2\text{O}$ ,<sup>[4]</sup> which forms a CsCl (**bcu**) topology net. The solvent molecules, which do not contribute to the net connectivity, are omitted for clarity. The net vertices are drawn at the centroid of each molecule of **1**.

Colour code: C, white; H, pale grey; O, red.

The local hydrogen bonding arrangement about each molecule of **1** is shown in Fig. 1 of the main article.



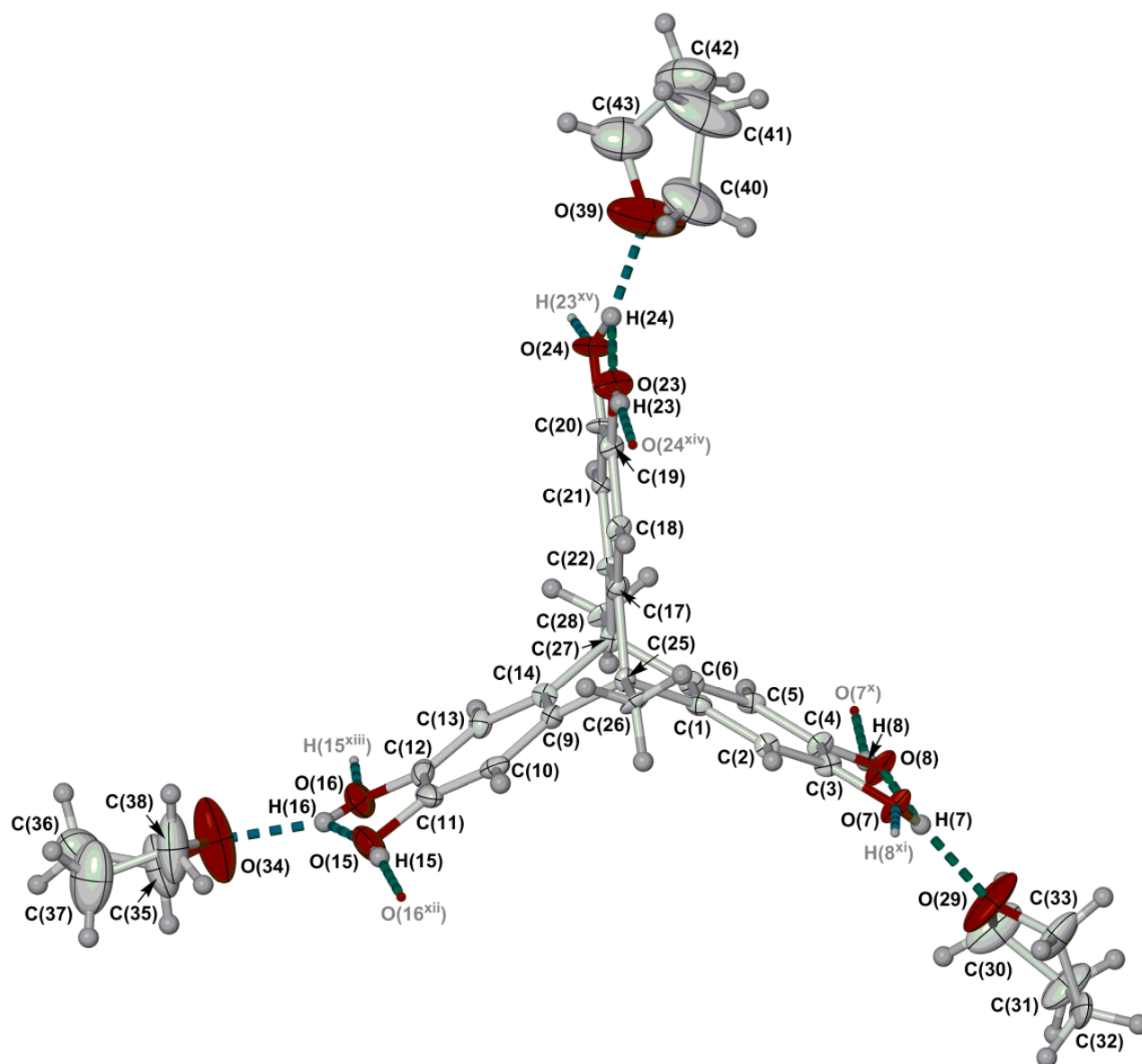


**Fig. S4.** View of the asymmetric unit in the crystal structure of **1·3.4thf**.

Displacement ellipsoids are at the 50 % probability level, except for H atoms which have arbitrary radii.

Colour code: C, white; H, pale grey; O, red. Symmetry codes: (x)  $1-x, 1-y, -1/2+z$ ; (xi)  $1-x, 1-y, 1/2+z$ ; (xii)  $x, x-y, 1/2+z$ ; (xiii)  $x, x-y, -1/2+z$ ; (xiv)  $-x+y, y, 1/2+z$ ; (xv)  $-x+y, y, -1/2+z$ .

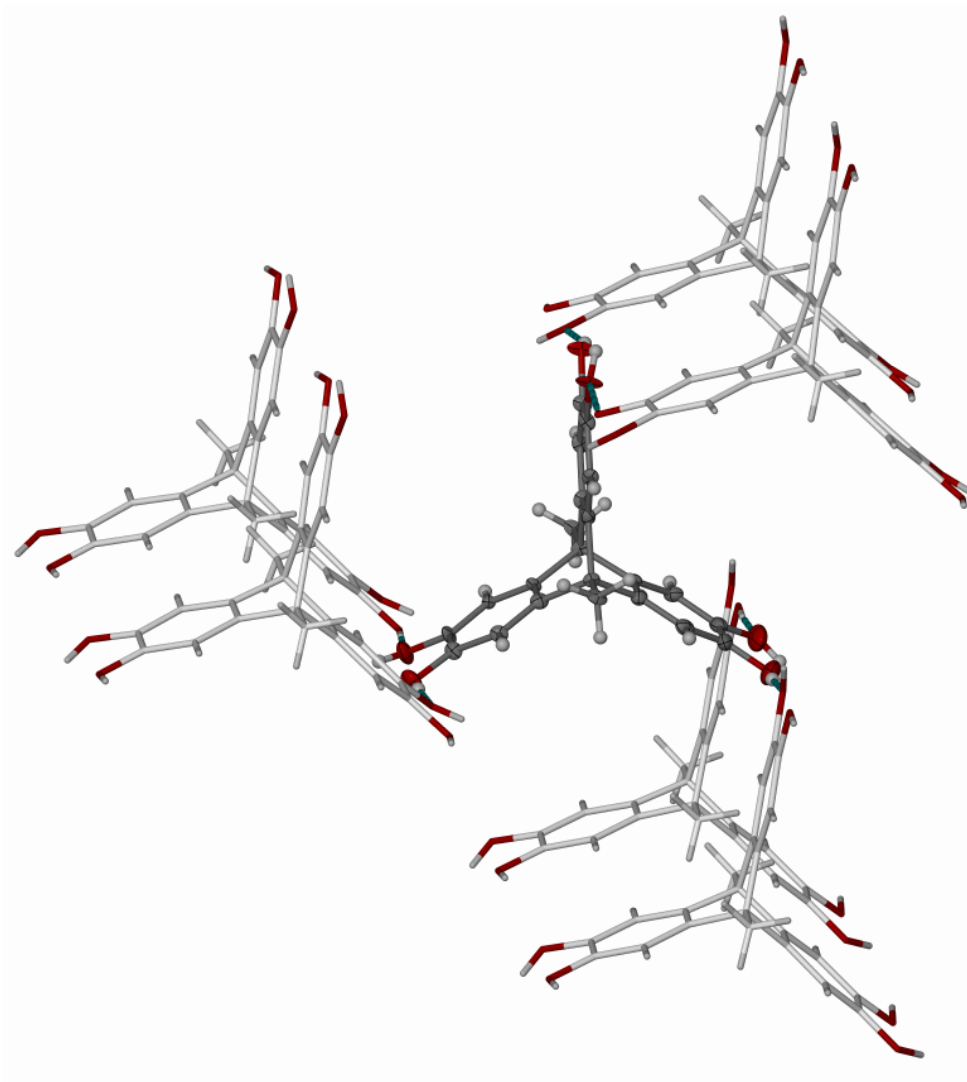


**Fig. S5.** Packing diagram of **1**·3.4thf, showing each molecule of **1** hydrogen bonding to six nearest neighbours in an approximately trigonal prismatic array. The three thf molecules in the model accept hydrogen bonds from **1** but do not contribute to the network connectivity, and so have been omitted for clarity.

Colour code: C, white; H, pale grey; O, red.

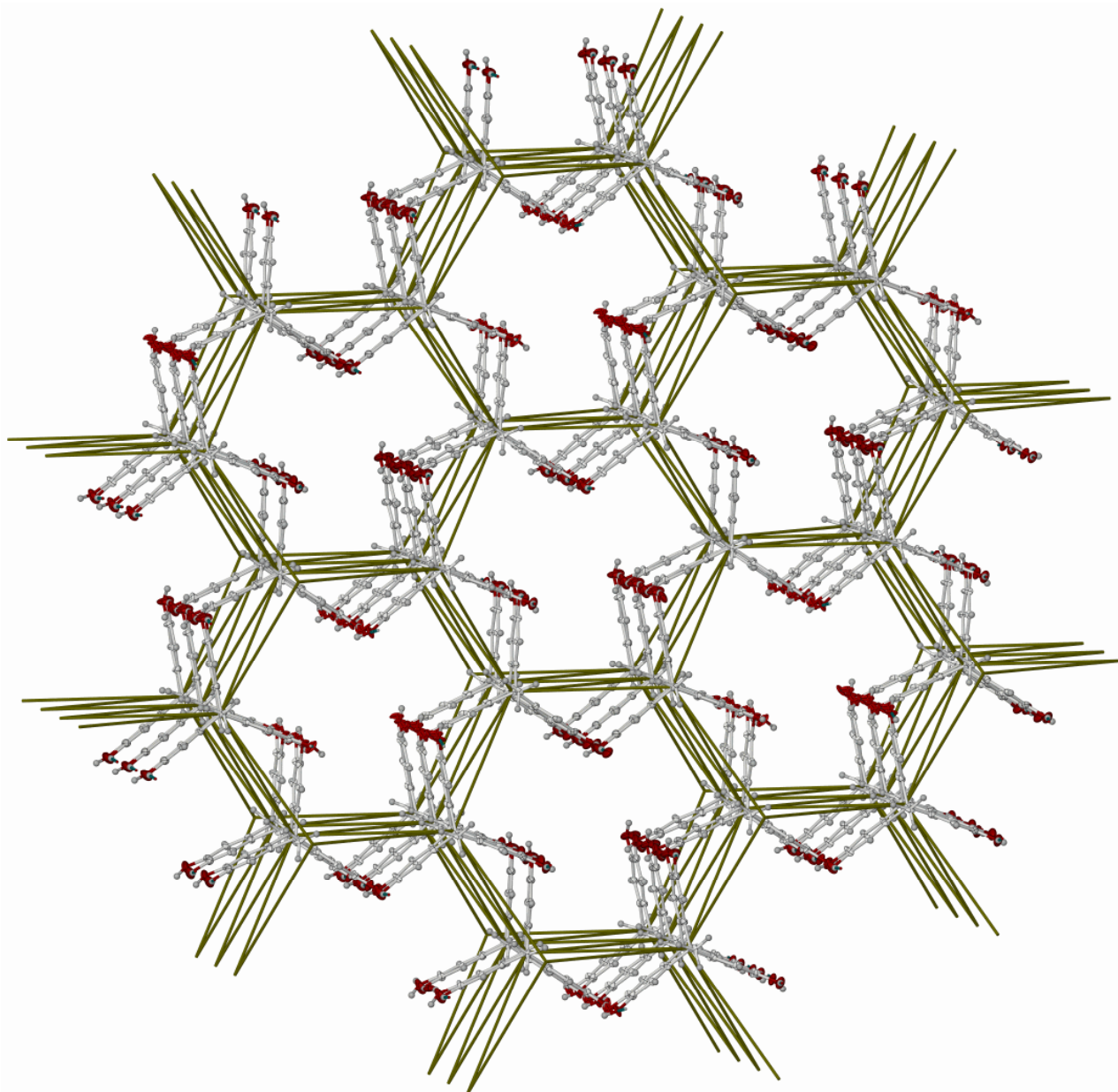


**Fig. S6.** Figure showing the hydrogen bonding connectivity in **1**·3.4thf, which forms a  $4^9_6$  (**acs**) topology net. The solvent molecules, which do not contribute to the net connectivity, are omitted for clarity. The net vertices are drawn at the centroid of each molecule of **1**.

Colour code: C, white; H, pale grey; O, red.

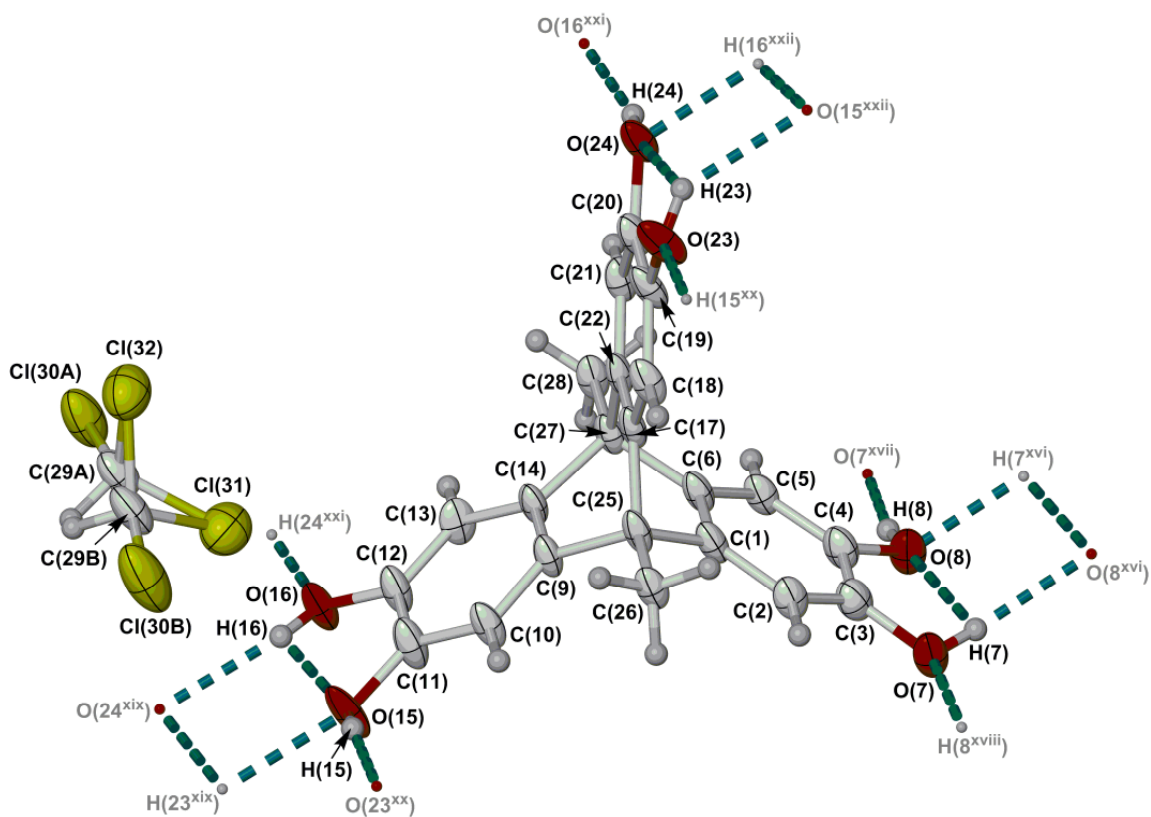


**Fig. S7.** View of the asymmetric unit in the crystal structure of  $1 \cdot 2.15\text{CHCl}_3$ .

Both equally occupied orientations of the disordered chloroform molecule are shown. Displacement ellipsoids are at the 50 % probability level, except for H atoms which have arbitrary radii.

Colour code: C, white; H, pale grey; Cl, yellow; O, red. Symmetry codes: (xvi)  $1-x, 1-y, 2-z$ ;  
(xvii)  $x, 1-y, 1/2+z$ ; (xviii)  $x, 1-y, -1/2+z$ ; (xix)  $-1/2+x, 1/2-y, -1/2+z$ ; (xx)  $1/2-x, 1/2-y, 1-z$ ;  
(xxi)  $1/2-x, 1/2-y, 2-z$ ; (xxii)  $1/2+x, 1/2-y, 1/2+z$ .

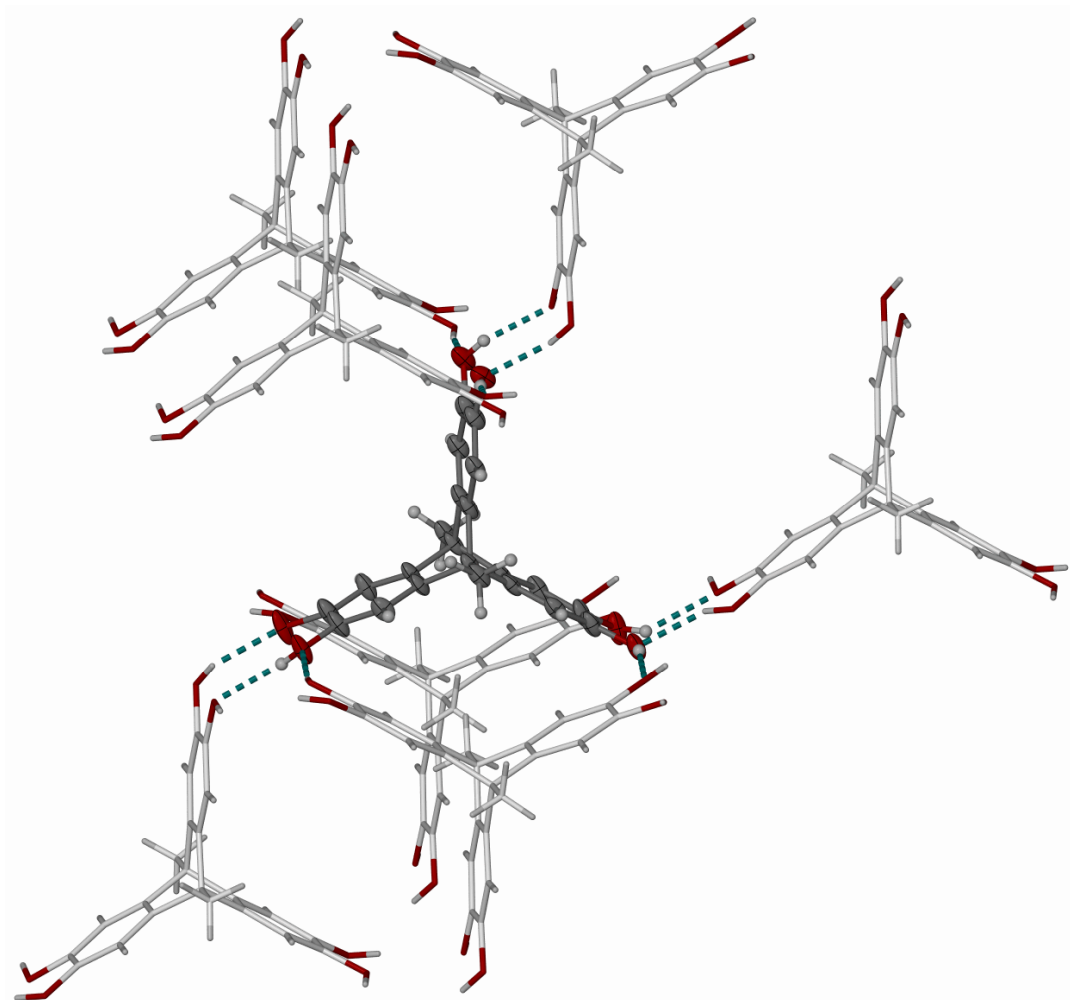


**Fig. S8.** Packing diagram of **1**·2.15CHCl<sub>3</sub>, showing each molecule of **1** hydrogen bonding to seven nearest neighbours. The chloroform solvent molecules do not take part in hydrogen bonding, and are omitted for clarity.

Colour code: C, white; H, pale grey; O, red.

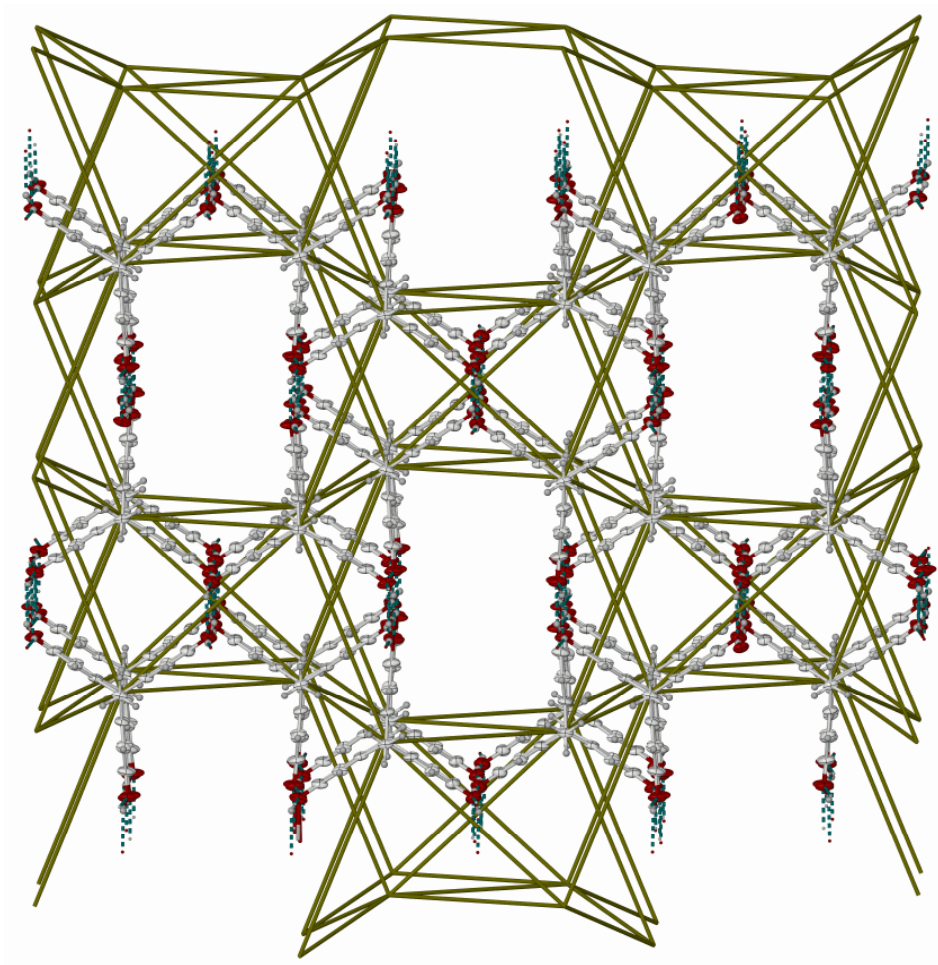


**Fig. S9.** Figure showing the seven-connected hydrogen bonded net in  $\mathbf{1} \cdot 2.15\text{CHCl}_3$ . The solvent molecules, which do not contribute to the net connectivity, are omitted for clarity. The net vertices are drawn at the centroid of each molecule of  $\mathbf{1}$ .



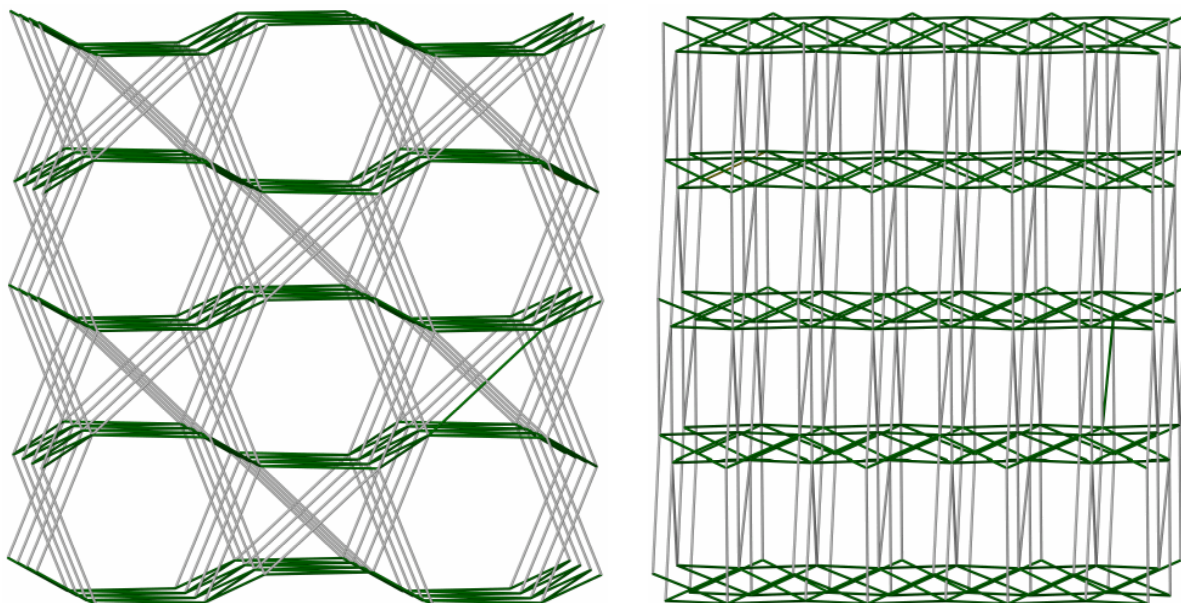


**Fig. S10.** Two views of the seven-connected hydrogen bonded net in **1**·2.15CHCl<sub>3</sub> (Fig. S9), emphasising its relationship to stacks of puckered 4<sup>4</sup> sheets (green) linked by addition pillaring connections (pale grey). The net vertices are drawn at the centroid of each molecule of **1**.

The net is formed from multiple 4- and 6-membered rings; there are no three-membered circuits. We are unaware of any other examples of this network topology in molecular or coordination framework crystals, but close variants of this net with different patterns of pillaring connections are known.<sup>[6,7]</sup>



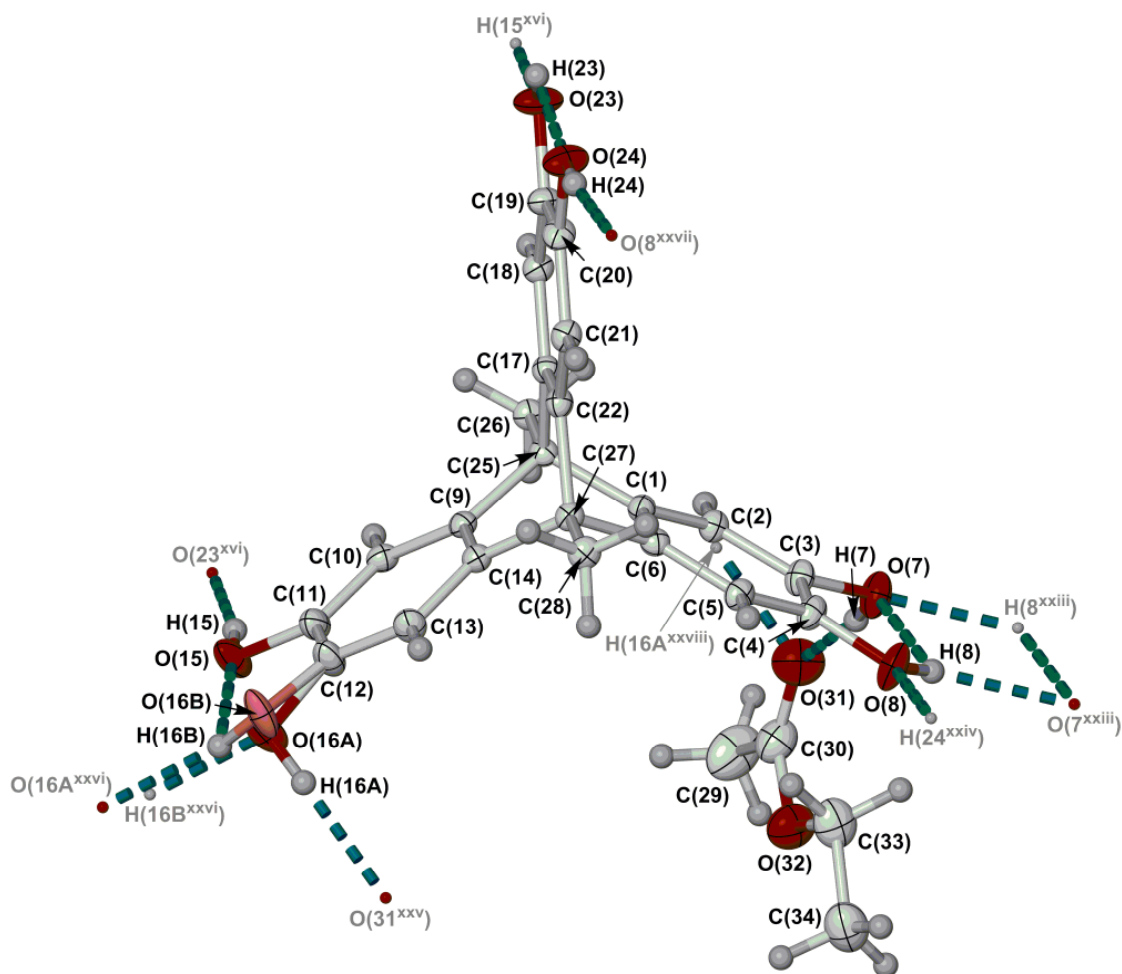


**Fig. S11.** View of the asymmetric unit in the crystal structure of **1**·EtOAc.

Displacement ellipsoids are at the 50 % probability level, except for H atoms which have arbitrary radii. Both orientations of the disordered hydroxyl group O(16)/H(16) are shown, with the 'B' orientation having paler colouration for clarity.

Colour code: C, white; H, pale grey; O, red. Symmetry codes: (xvi)  $1-x, 1-y, 2-z$ ; (xxiii)  $-x, 2-y, 1-z$ ; (xxiv)  $1-x, 1-y, 1-z$ ; (xxv)  $x, -1+y, z$ ; (xxvi)  $-x, -y, 2-z$ ; (xxvii)  $1-x, 1-y, 1-z$ ; (xxviii)  $x, 1+y, z$ .

The hydroxyl group disorder arises because of a hydrogen bond between O(16) and its symmetry equivalent related by  $-x, -y, 2-z$ , which must be disordered about the crystallographic inversion center.

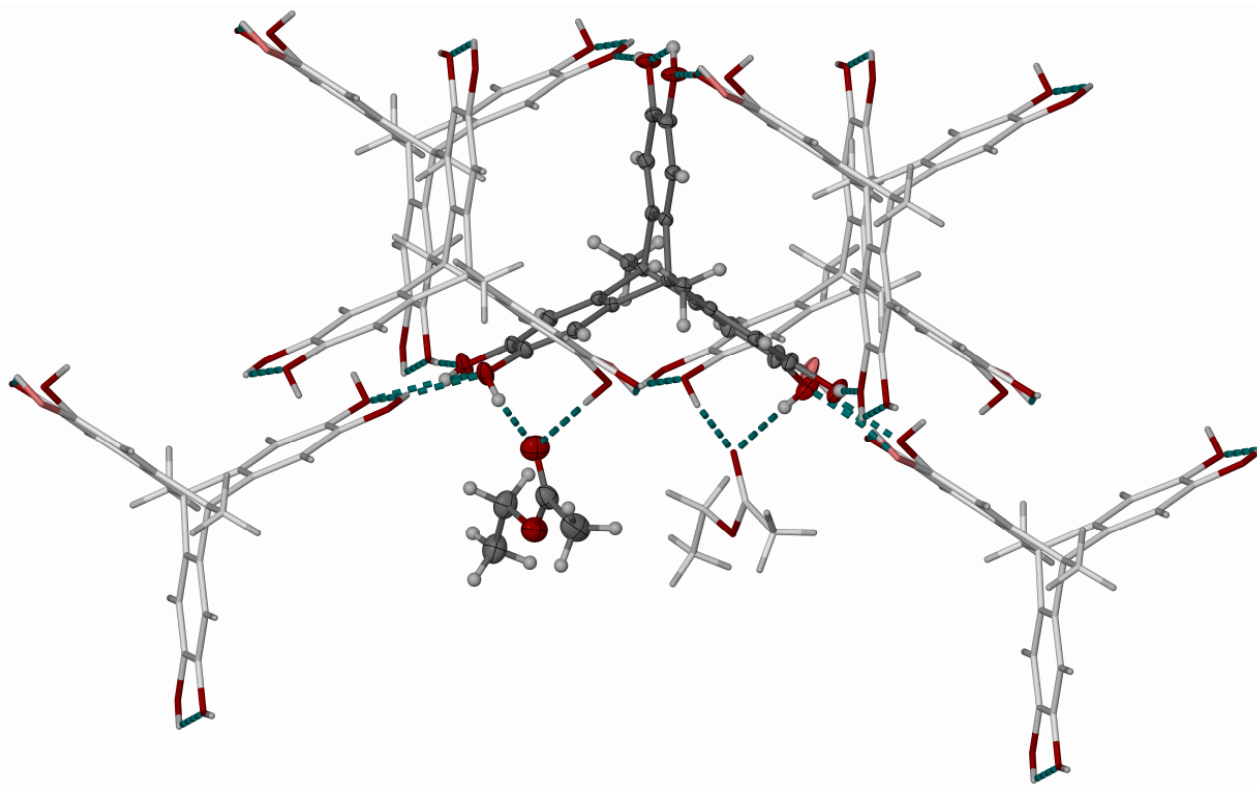


**Fig. S12.** Packing diagram of **1**·EtOAc, showing each molecule of **1** connecting to six nearest neighbours either directly, or *via* the solvent molecule which is a linear topological linker. Both orientations of the disordered hydroxyl group O(16)/H(16) are shown, with the 'B' orientation having paler colouration for clarity (*c.f.* Fig. S11).

Colour code: C, white; H, pale grey; O, red.

Three of the six network connections to the molecule involve disordered, half-occupied hydrogen bonds (Fig. S14).

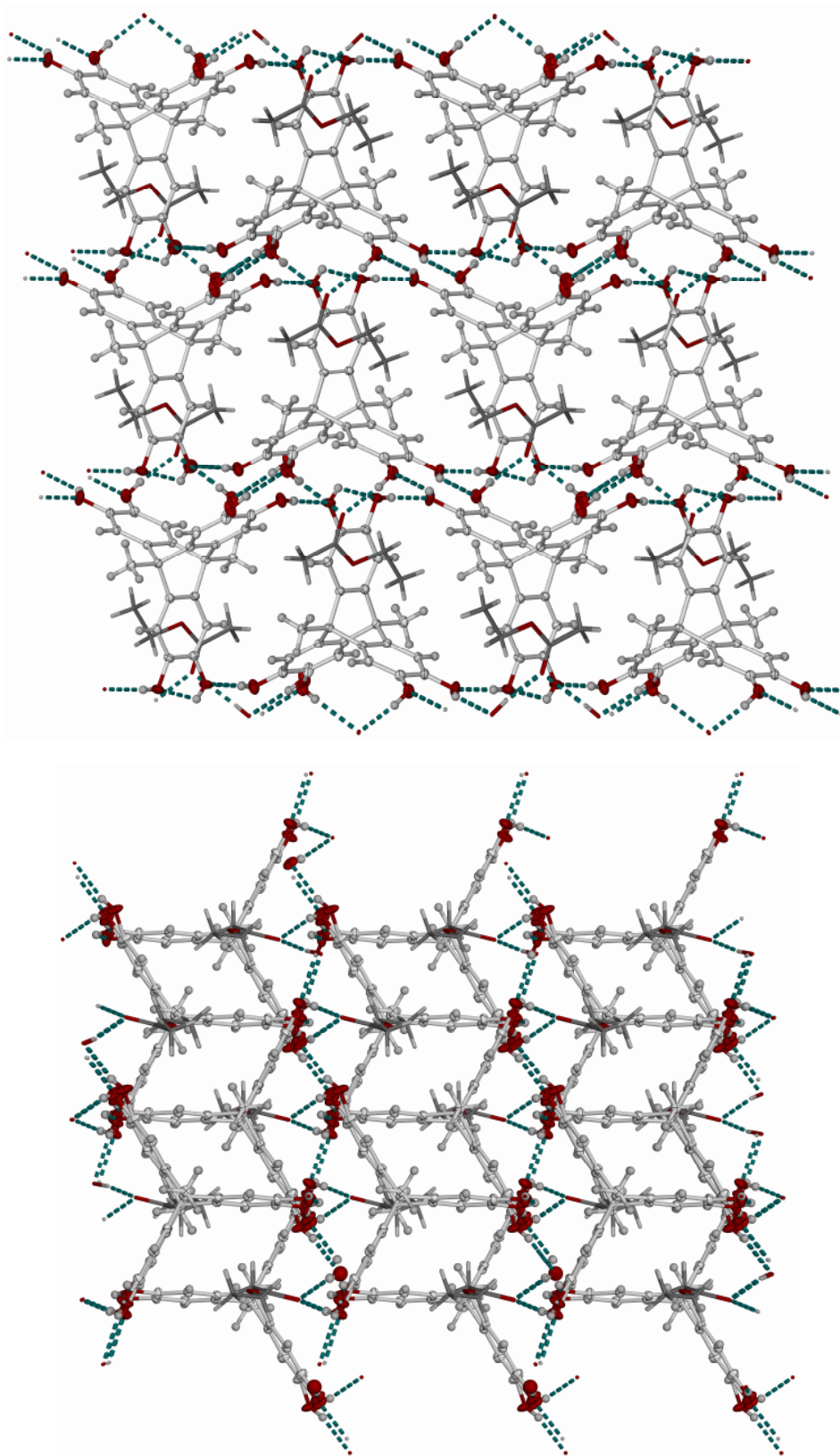


**Fig. S13.** Packing diagrams of **1**·EtOAc. The views are parallel to (010) with *c* horizontal (top), and parallel to (011) with *a* horizontal (bottom). Atomic displacement ellipsoids are at the 50 % probability level (for **1**) or with arbitrary atomic radii (solvent).

Colour code: C (**1**), white; C (solvent), dark grey; H, pale grey; O, red.

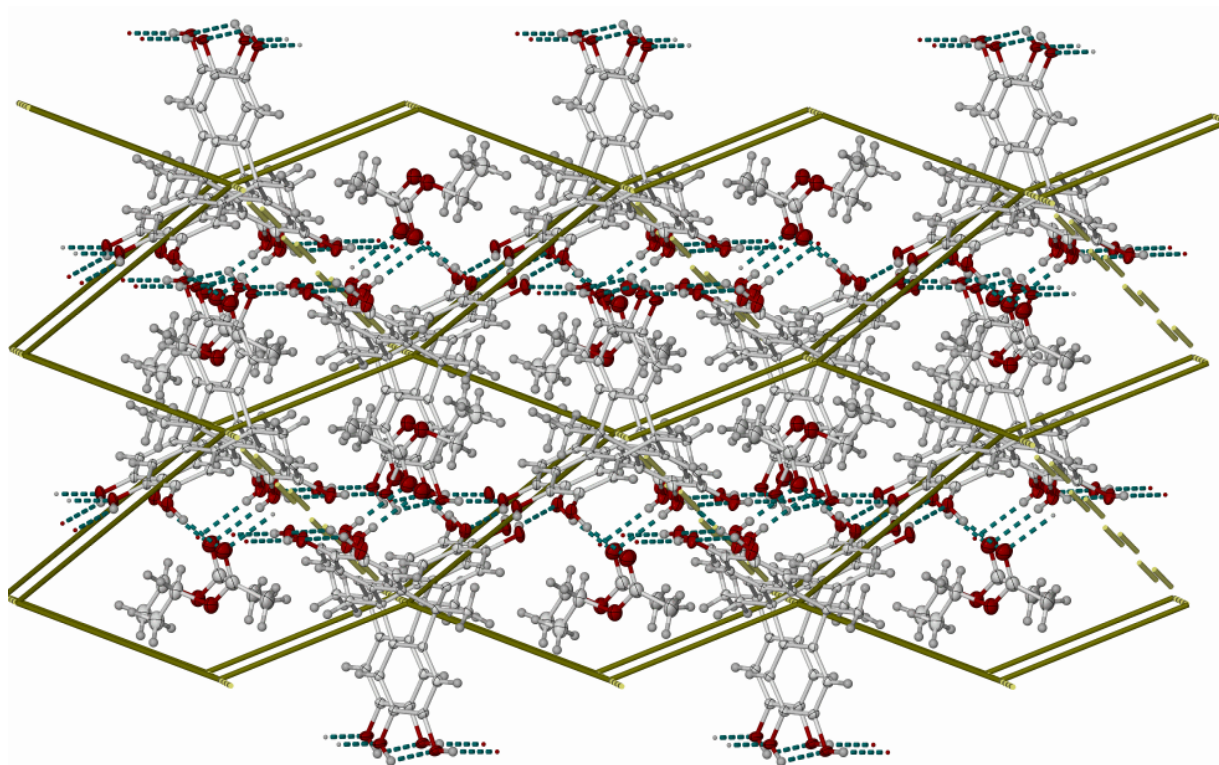


**Fig. S14.** Figure showing the hydrogen bonded net connectivity in **1**·EtOAc. The crystallographically disordered connections are shown as dashed pale yellow lines.

Colour code: C, white; H, pale grey; O, red.

The ordered (solid, dark yellow) connections form puckered  $6^3$  sheets along the  $[\bar{1} 11]$  plane. The disordered (dashed, pale yellow) connections link these 2D arrays into 3D, forming a six-connected **bsn** net if all the connections are considered equally. The **bsn** topology resembles a helical  $4^4$  array<sup>[8]</sup> with neighbouring helices having opposite handedness.

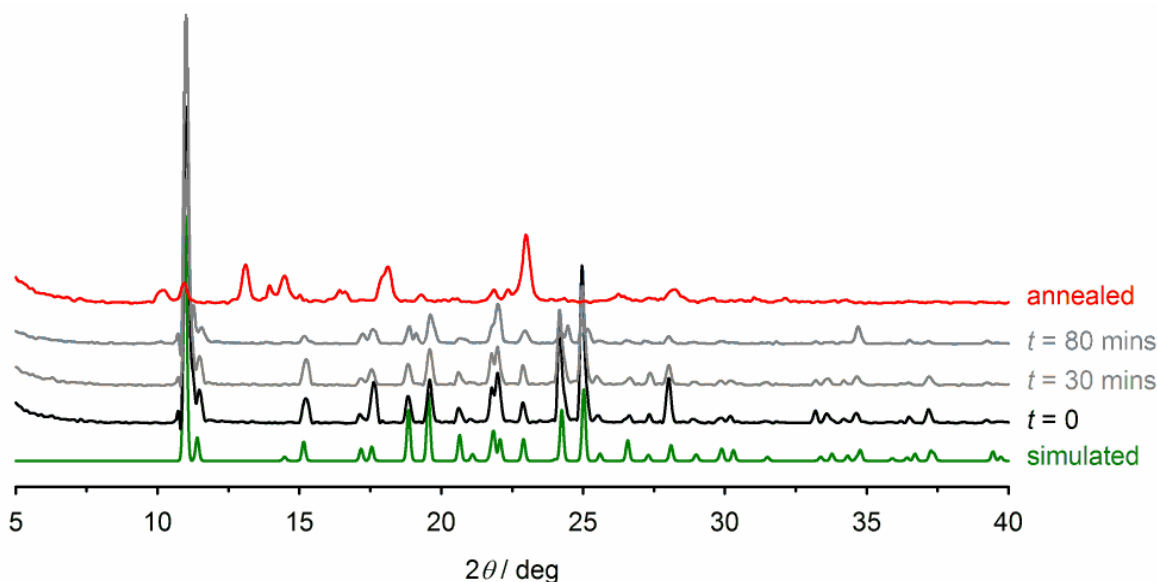


**Fig. S15.** X-ray powder diffraction data from **1**·2Et<sub>2</sub>O at 293 K, including a simulated powder pattern based on the crystal structure of that compound. The sample was measured as-isolated ( $t = 0$ ); after 30 and 80 minutes standing at room temperature; then after annealing for 30 minutes at 370 K.

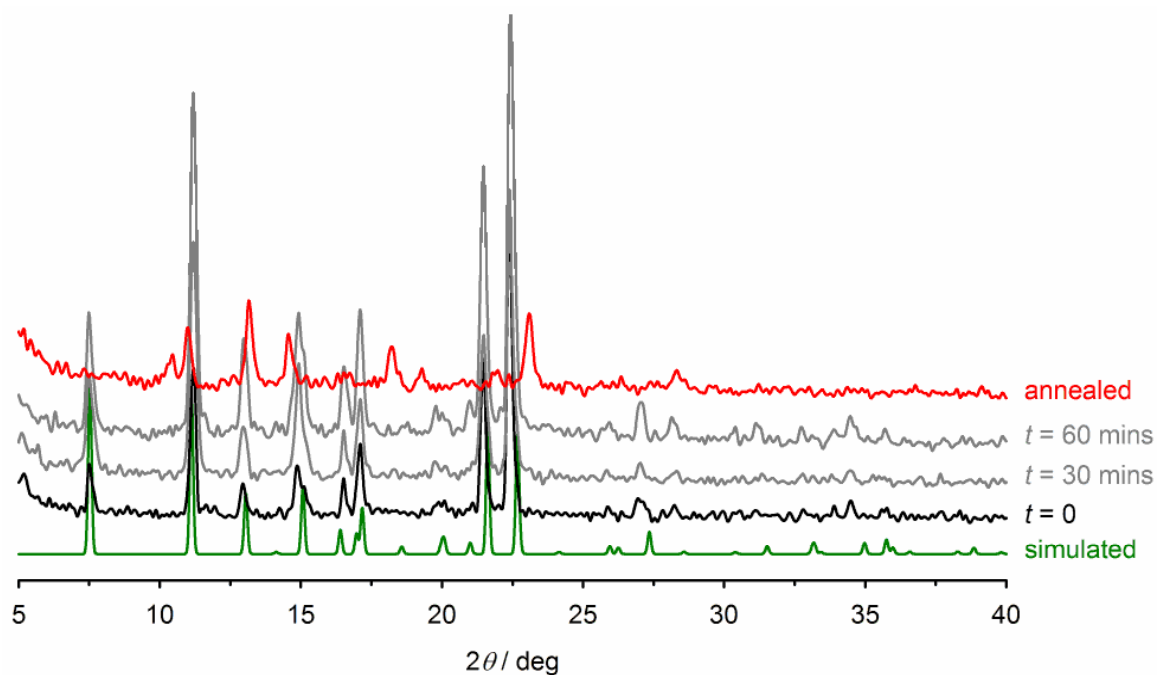


**Fig. S16.** X-ray powder diffraction data from **1**·3.4thf at 293 K, including a simulated powder pattern based on the crystal structure of that compound. The sample was measured as-isolated ( $t = 0$ ); after 30 and 60 minutes standing at room temperature; then after annealing for 30 minutes at 370 K.

Both samples are phase pure, but slowly lose their crystallinity upon standing in air. The annealing process transforms them to a new phase, **1'**, which we have not characterized crystallographically but is presumably solvent-free **1**.

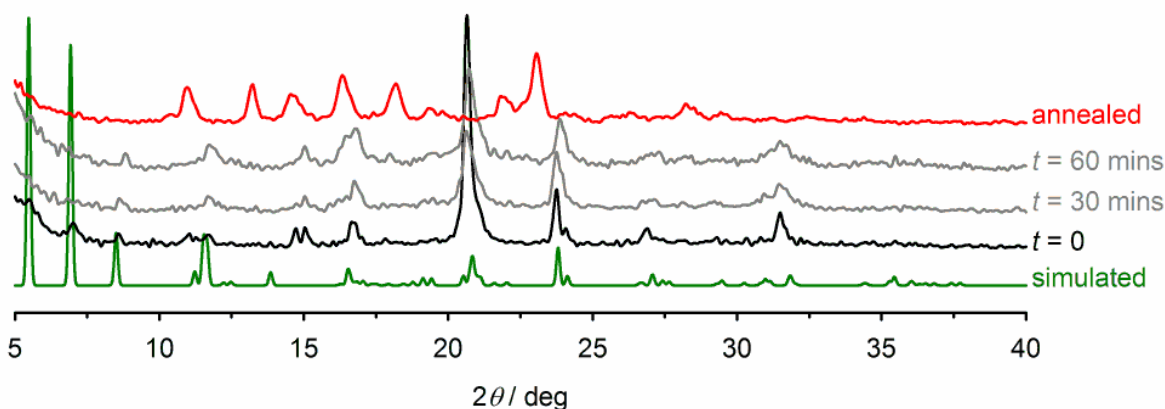


**Fig. S17.** X-ray powder diffraction data from  $1 \cdot 2.15\text{CHCl}_3$  at 293 K, including a simulated powder pattern based on the crystal structure of that compound. The sample was measured as-isolated ( $t = 0$ ); after 30 and 60 minutes standing at room temperature; then after annealing for 30 minutes at 370 K.

The sample is poorly crystalline, possibly from solvent loss inside the diffractometer, and the patterns show preferred orientation effects. None-the-less the agreement with the simulated pattern is good, apart from an observed pair of peaks at  $2\theta = 15^\circ$  that are not reproduced in the powder pattern. Those peaks could arise from the unmodelled contents of the large pores in the crystalline asymmetric unit.

The behaviour of the sample upon standing in air (further peak broadening) and annealing (transformation to  $1'$ ) is the same as for  $1 \cdot 2\text{Et}_2\text{O}$  and  $1 \cdot 3.4\text{thf}$  (Figs. S15 and S16).

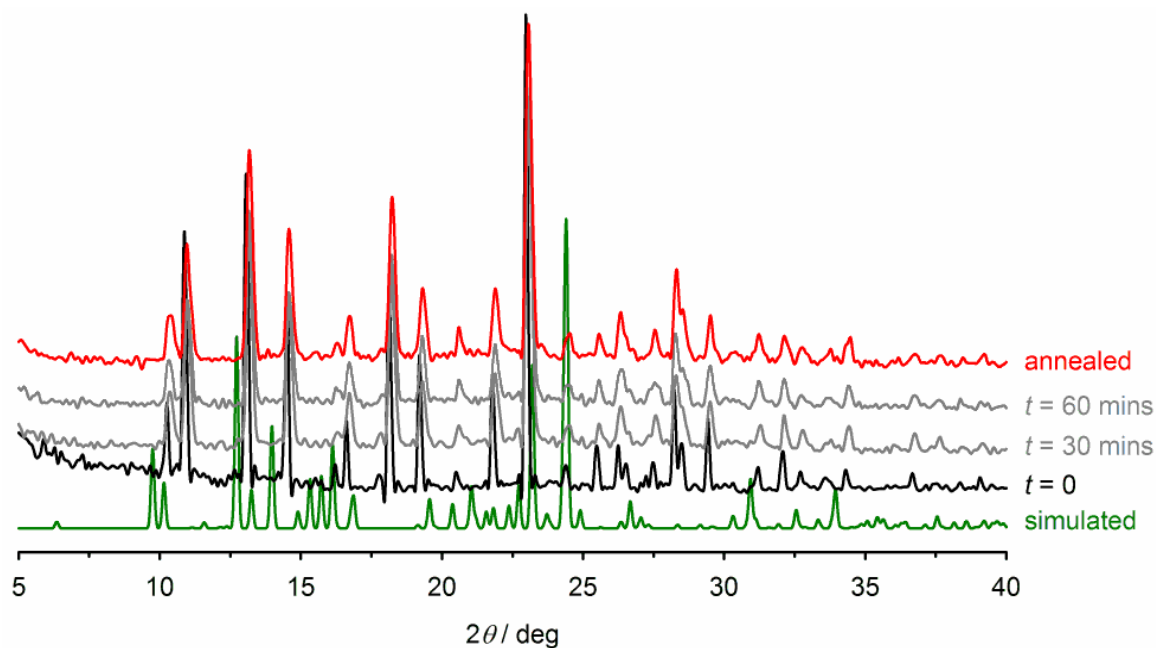


**Fig. S18.** X-ray powder diffraction data from a microcrystalline sample of  $1$  crystallized from ethyl acetate/pentane, including a simulated powder pattern based on the crystal structure obtained from that solvent mixture,  $1 \cdot \text{EtOAc}$ . The sample was measured as-isolated ( $t = 0$ ); after 30 and 60 minutes standing at room temperature; then after annealing for 30 minutes at 370 K.

In contrast to the other solvates, this sample of  $1$  does not match the simulated pattern from  $1 \cdot \text{EtOAc}$ , and instead apparently contains the pure  $1'$  phase. This is unchanged upon annealing, apart from some minor peak broadening.

**Table S3** Hydrogen bond parameters for the crystal structures of **2** (Å, °).<sup>a</sup> See Figs. S19 and S23 for the atom numbering scheme for each structure.

	D–H	H...A	D...A	D–H...A
<b>2</b> ·½Et <sub>2</sub> O·½H <sub>2</sub> O <sup>[4]</sup>				
O(7)–H(7)...O(8)	0.897(19)	2.25(4)	2.674(3)	108(3)
O(7)–H(7)...O(15 <sup>xxviii</sup> )	0.897(19)	2.23(3)	3.057(3)	153(4)
O(8)–H(8)...O(34)	0.911(19)	1.82(2)	2.728(3)	175(4)
O(15)–H(15)...O(58B <sup>xxx</sup> )	0.890(19)	2.26(3)	3.087(8)	154(4)
O(16)–H(16)...O(15)	0.894(19)	2.24(4)	2.713(4)	113(3)
O(33)–H(33)...O(34)	0.89(2)	2.32(5)	2.718(4)	107(4)
O(33)–H(33)...O(7 <sup>xxix</sup> )	0.89(2)	1.96(3)	2.744(3)	146(5)
O(34)–H(34)...O(41 <sup>xxxii</sup> )	0.890(19)	1.76(2)	2.650(4)	175(5)
O(41)–H(41)...O(42)	0.91(2)	2.27(5)	2.675(4)	107(3)
O(41)–H(41)...O(16 <sup>xxxii</sup> )	0.91(2)	1.96(3)	2.726(3)	140(4)
O(42)–H(42)...O(58A)/O(58B)	0.89(2)	1.82(2)/1.76(3)	2.707(5)/2.536(7)	176(5)/144(5)
O(58A)/O(58B)...O(33 <sup>xxxii</sup> )	–	–	2.822(5)/2.512(7)	–
O(58A)/O(58B)...O(55A)/O(55B)/O(55C)	–	–	2.325(5)–3.105(7)	–
<b>2</b> -dioxane				
O(7)–H(7)...O(15 <sup>xxxiv</sup> )	0.83(4)	1.92(4)	2.738(2)	168(4)
O(8)–H(8)...O(30 <sup>xxxv</sup> )	0.85(4)	1.89(4)	2.674(3)	153(3)
O(15)–H(15)...O(8 <sup>xxxvii</sup> )	0.82(4)	1.88(4)	2.692(2)	168(3)
O(16)–H(16)...O(27)	0.86(4)	1.89(4)	2.738(3)	168(3)
<sup>a</sup> Symmetry codes: (xxviii) $x, 1+y, z$ ; (xxix) $-x, 1-y, 1-z$ ; (xxx) $-1+x, 1/2-y, -1/2+z$ ; (xxxii) $1-x, 1/2+y, 3/2-z$ ; (xxxv) $3/2-x, 1-y, 1/2+z$ ; (xxxvi) $3/2-x, 2-y, 1/2+z$ ; (xxxviii) $1/2+x, 3/2-y, 1-z$ .				



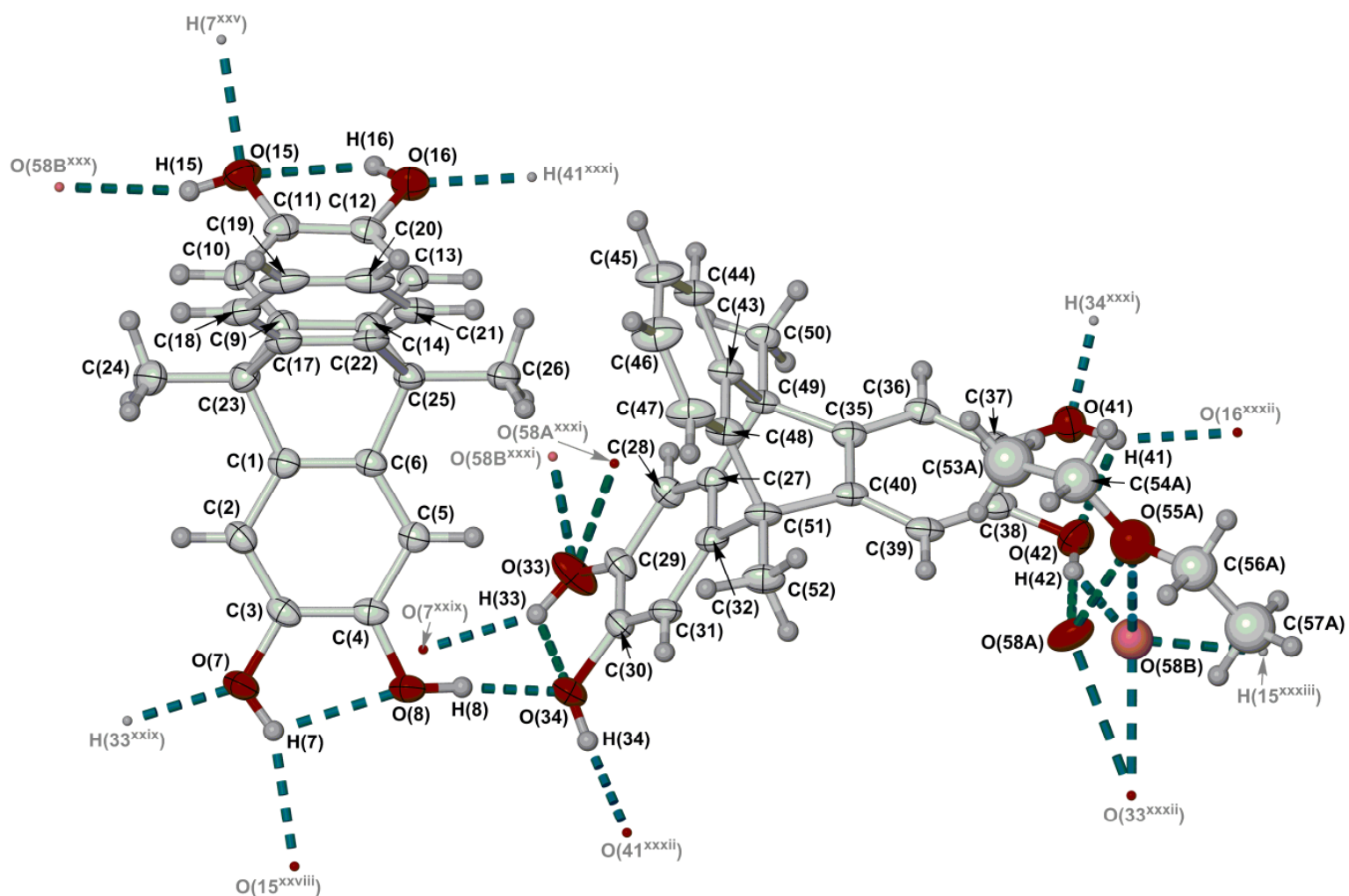


**Fig. S19.** View of the asymmetric unit in the crystal structure of  $2 \cdot \frac{1}{2} \text{Et}_2\text{O} \cdot \frac{1}{2} \text{H}_2\text{O}$ .<sup>[4]</sup>

Displacement ellipsoids are at the 50 % probability level, except for H atoms which have arbitrary radii. Only the major orientation of the disordered diethyl ether molecule is included, for clarity. Both orientations of the water site O(58) are shown, with the ‘B’ orientation having paler colouration.

Colour code: C, white; H, pale grey; O, red. Symmetry codes: (xxv)  $x, -1+y, z$ ; (xxviii)  $x, 1+y, z$ ; (xxix)  $-x, 1-y, 1-z$ ; (xxx)  $-1+x, \frac{1}{2}-y, -\frac{1}{2}+z$ ; (xxxi)  $1-x, -\frac{1}{2}+y, \frac{3}{2}-z$ ; (xxxii)  $1-x, \frac{1}{2}+y, \frac{3}{2}-z$ ; (xxxiii)  $1+x, \frac{1}{2}-y, \frac{1}{2}+z$ .

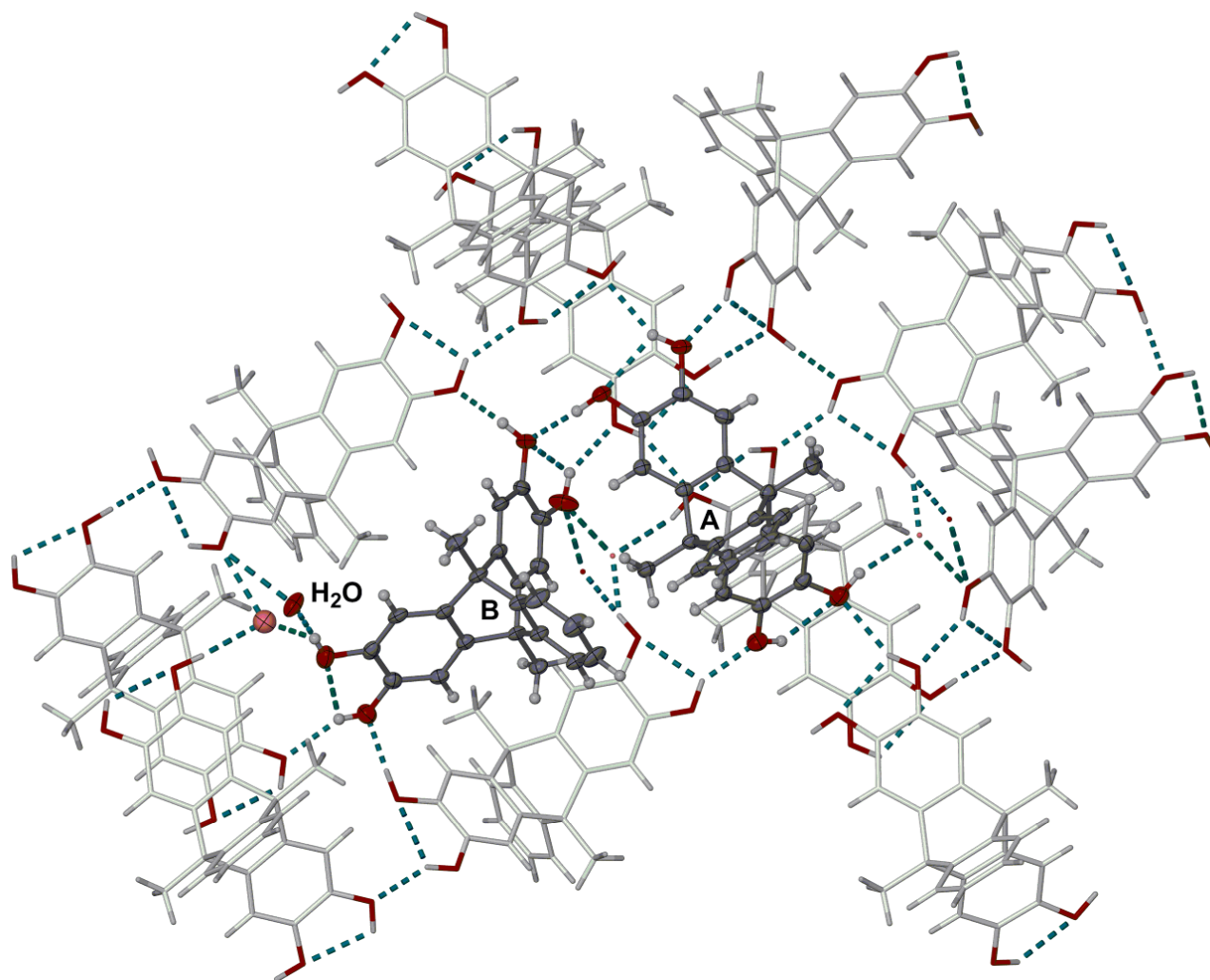


**Fig. S20.** Packing diagram of  $2 \cdot \frac{1}{2}\text{Et}_2\text{O} \cdot \frac{1}{2}\text{H}_2\text{O}$ ,<sup>[4]</sup> showing the hydrogen bonding interactions in the lattice. The diethyl ether molecule does not contribute to the network topology, and has been omitted for clarity. The disordered water molecule is either two- [O(58A), dark red] or three-connected [O(58B), pale red] by hydrogen bonding. Thus, molecule A of **2** [C(1)-C(26), Fig. S15] is either five or six-connected, and molecule B [C(27)-C(52)] can be five, six or seven-connected, depending on the disorder occupancy of its neighbouring water sites.

Colour code: C, dark grey or white; H, pale grey; O, red.

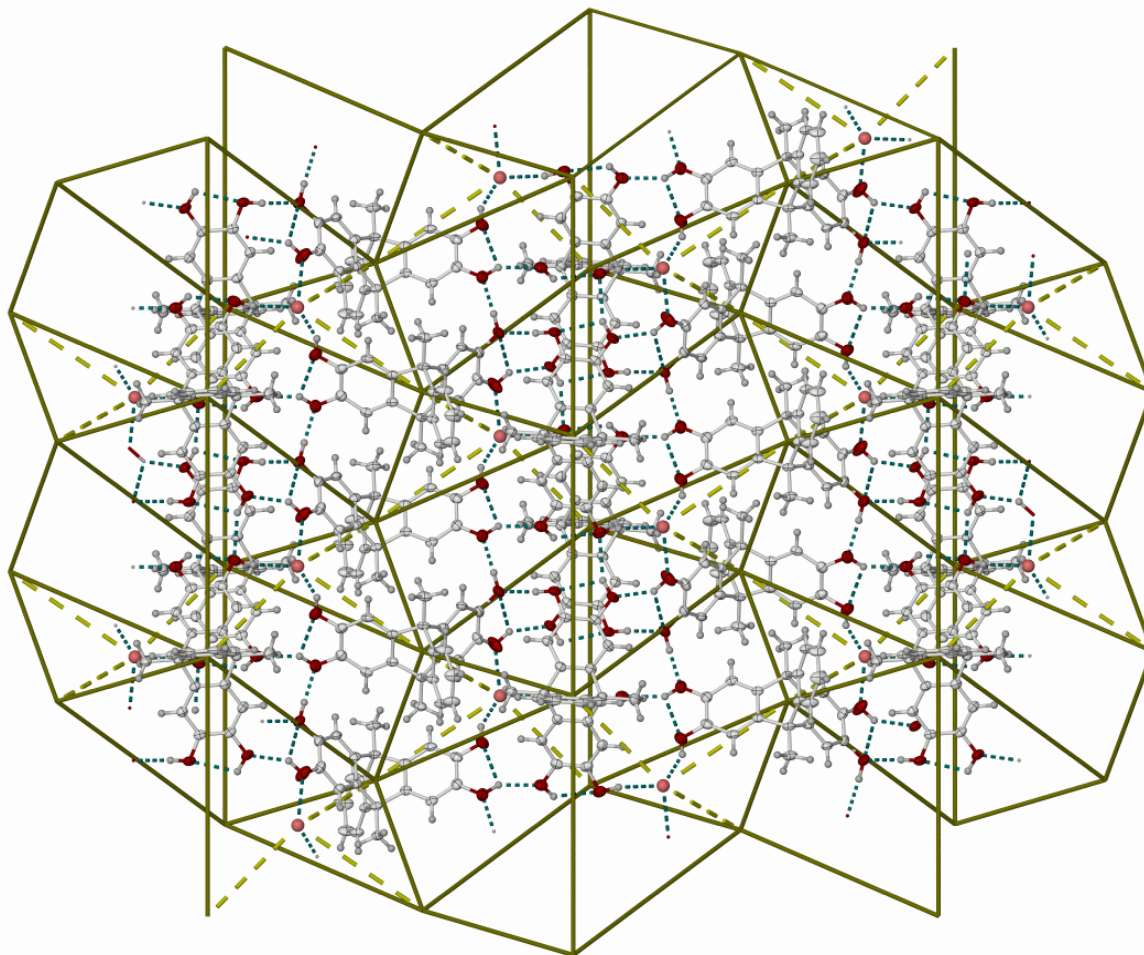


**Fig. S21.** Figure showing the 2D bilayer hydrogen bonded net in  $2 \cdot \frac{1}{2}\text{Et}_2\text{O} \cdot \frac{1}{2}\text{H}_2\text{O}$ .<sup>[4]</sup> The view is approximately perpendicular to the  $[10\bar{2}]$  plane. The net vertices are drawn at the centroid of each molecule of **2**, or to the water O atom (58B). The connections to the water molecule are all part-occupied because of its disorder (Fig. 20), and are shown as dashed pale yellow lines.

Colour code: C, white; H, pale grey; O (**2**), dark red; O (H<sub>2</sub>O), pale red.

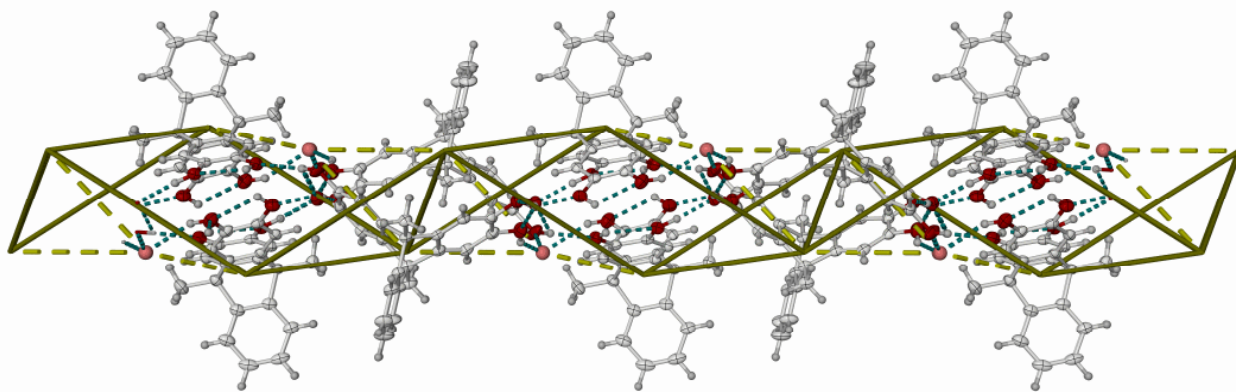


**Fig. S22.** Alternative view of the 2D bilayer hydrogen bonded net in  $2 \cdot \frac{1}{2}\text{Et}_2\text{O} \cdot \frac{1}{2}\text{H}_2\text{O}$ .<sup>[4]</sup> The view is parallel to the (010) crystal vector.

Colour code: C, white; H, pale grey; O (2), dark red; O (H<sub>2</sub>O), pale red.

The crystallographically ordered connections form a binodal five-connected net (Fig. S21), whose short Schläfli notation is  $3.5.4.3.4^2, 3.4^2.5^2.4.6$ . The disposition of connections around molecule B (Fig. S20) is approximately square pyramidal, but the connections around molecule A have a very irregular geometry.

The additional partial connections to the water site change the topology to a trinodal net with three, six and seven-connected nodes, if all the connections are considered equivalently.

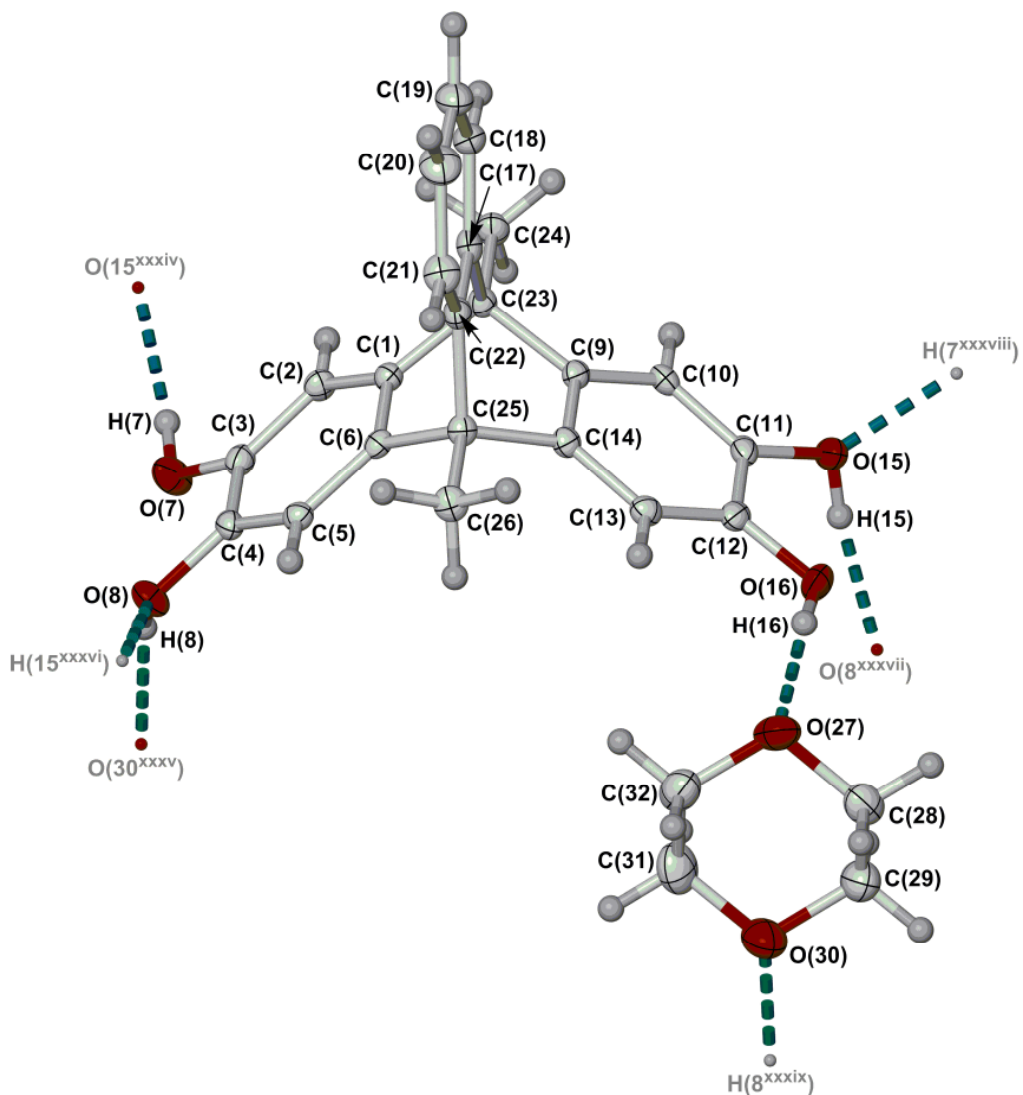


**Fig. S23.** View of the asymmetric unit in the crystal structure of **2**·dioxane.

Displacement ellipsoids are at the 50 % probability level, except for H atoms which have arbitrary radii. Both orientations of the disordered hydroxyl group O(16)/H(16) are shown, with the ‘B’ orientation having paler colouration for clarity.

Colour code: C, white; H, pale grey; O, red. Symmetry codes: (xxxiv)  $^{3/2-x}, 1-y, 1/2+z$ ;  
 (xxxv)  $^{3/2-x}, 2-y, 1/2+z$ ; (xxxvi)  $^{-1/2+x}, 3/2-y, 1-z$ ; (xxxvii)  $^{1/2+x}, 3/2-y, 1-z$ ; (xxxviii)  $^{3/2-x}, 1-y, -1/2+z$ ;  
 (xxxix)  $^{3/2-x}, 2-y, -1/2+z$ .

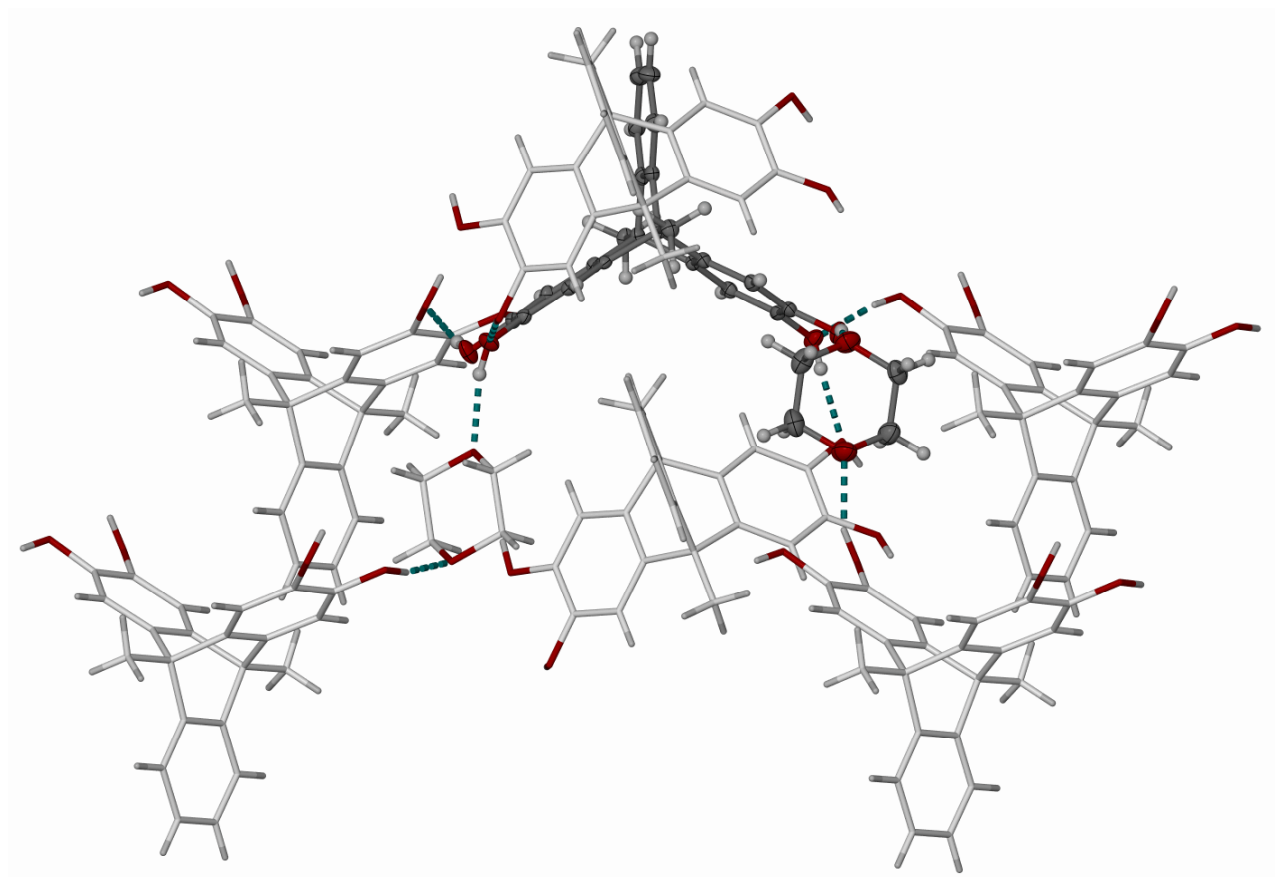


**Fig. S24.** Packing diagram of **2**-dioxane, showing each molecule of **2** connecting to an irregular array of six nearest neighbours, either directly or *via* the solvent molecule which is a linear topological linker.

Colour code: C, dark grey or white; H, pale grey; O, red.



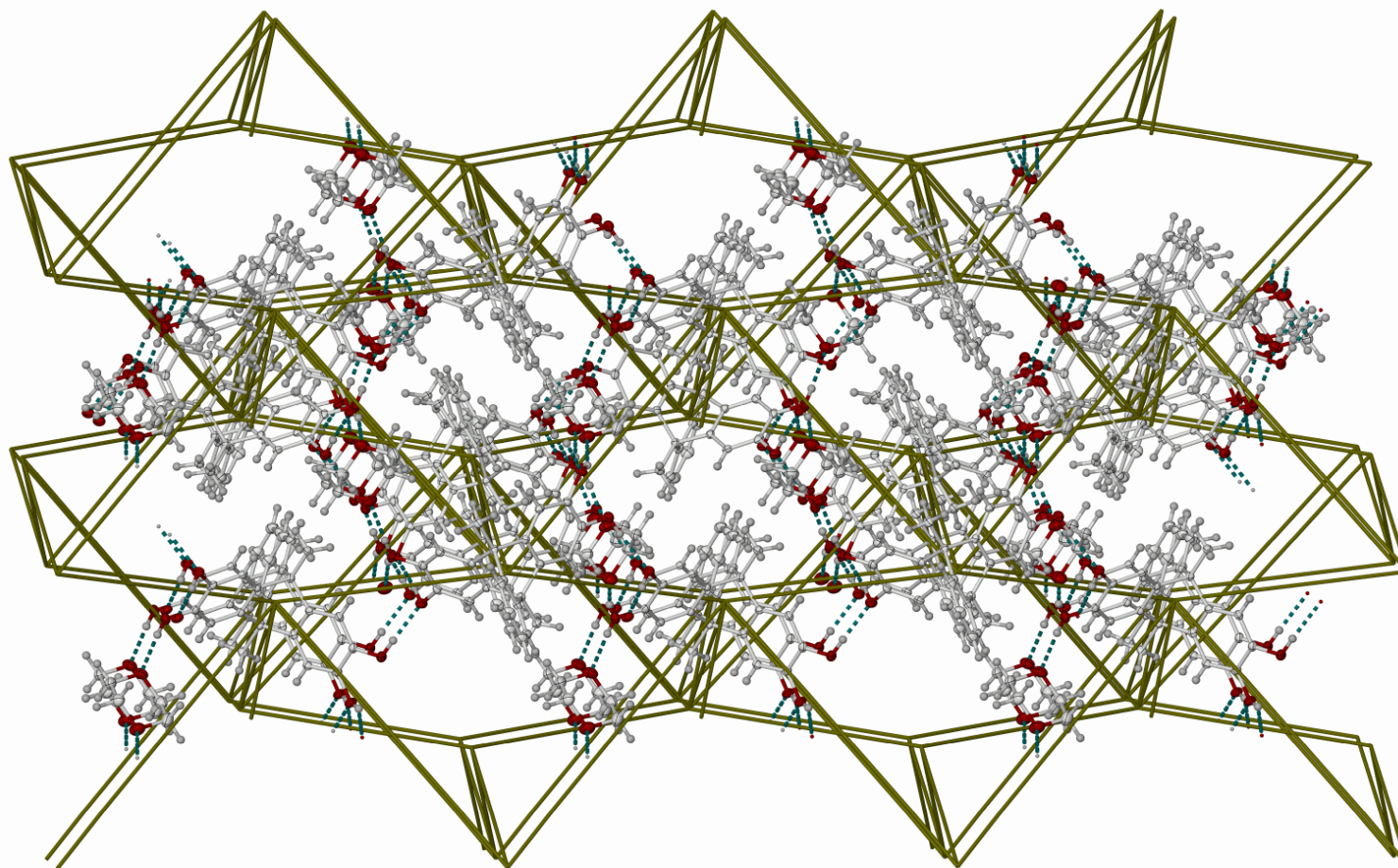


**Fig. S25.** Figure showing the six-connected hydrogen bonded net in **2**·dioxane. The net vertices are drawn at the centroid of each molecule of **2**.

Colour code: C, white; H, pale grey; O, red.

The topology is based on a  $6^5.8$  (**dmp**) network which is modified by additional diagonal connections, *via* the bridging dioxane molecules, between six-membered rings in the net. By inspection, the short Schläfli symbol for this net would be  $4^{12}.6^n$ , where  $n \geq 50$ .



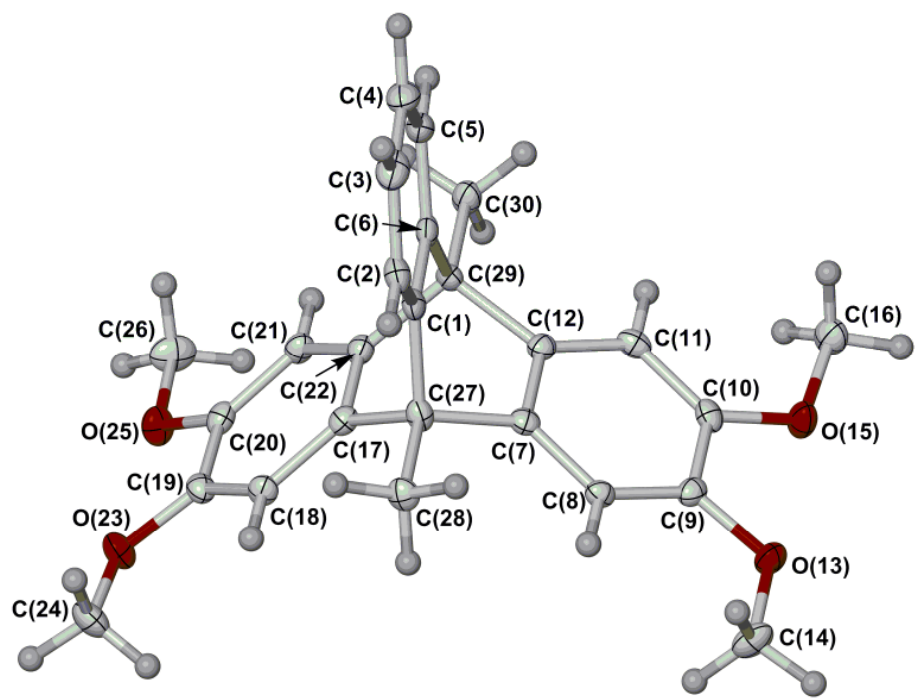


**Fig. S26.** View of the molecule in the crystal structure of **3**. Displacement ellipsoids are at the 50 % probability level, except for H atoms which have arbitrary radii.

Colour code: C, white; H, pale grey; O, red.

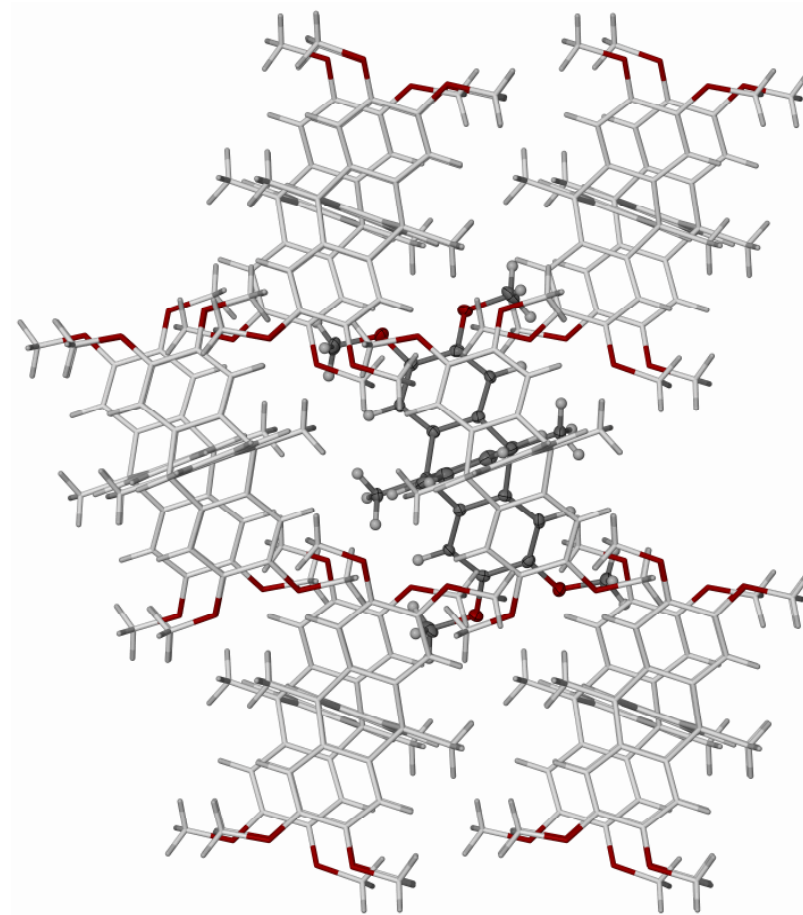
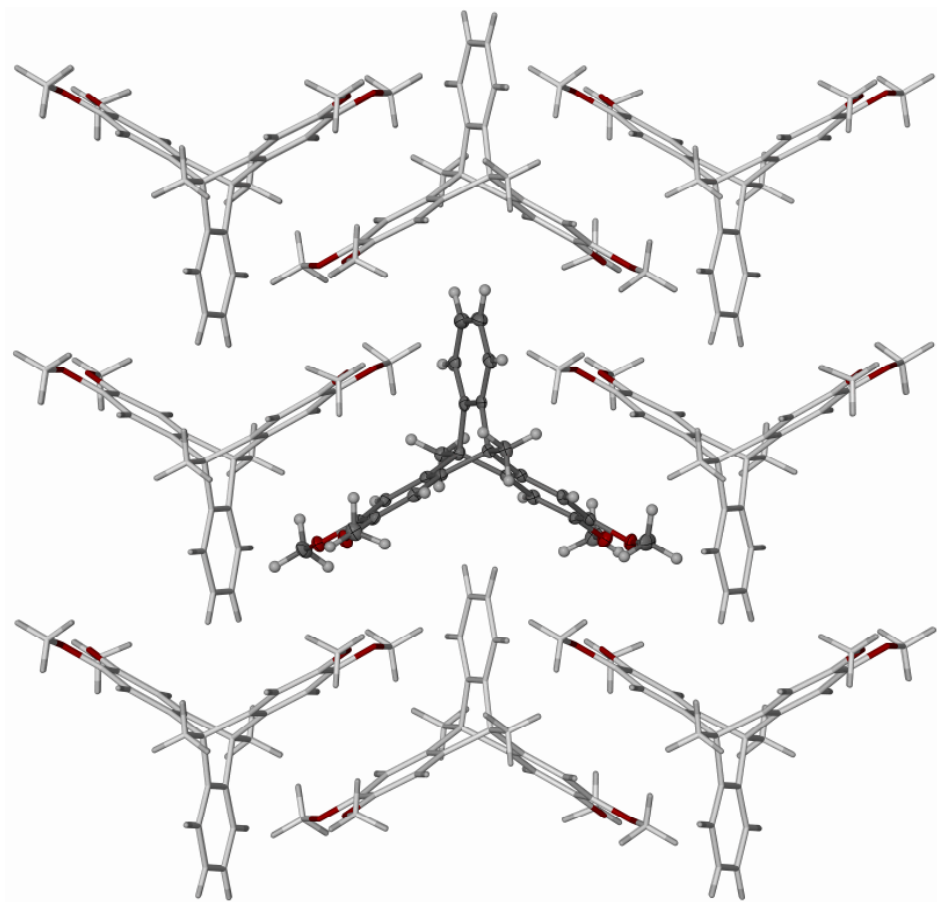


**Fig. S27.** Packing diagrams of **3**. The views are parallel to the crystallographic [100] vector (left), and the [001] vector (right). Other details as for Fig. S22.

Nearest neighbour molecules in the crystal are offset along  $a$ , and canted, with respect to each other. So, despite the appearance of the diagrams, there are no  $\pi \dots \pi$  interactions between molecules in the lattice.

## References

1. G. M. Sheldrick, *Acta Crystallogr., Sect. A*, 2008, **64**, 112
2. L. J. Barbour, *J. Supramol. Chem.*, 2001, **1**, 189.
3. POVRAY, v. 3.5, Persistence of Vision Raytracer Pty. Ltd., Williamstown, Victoria, Australia, 2002. <http://www.povray.org>.
4. Y. Han, Y. Jiang and C.-F. Chen, *Chin. Chem. Lett.*, 2013, **24**, 475.
5. A. L. Spek, *J. Appl. Cryst.*, 2003, **36**, 7.
6. D.-L. Long, A. J. Blake, N. R. Champness, C. Wilson and M. Schröder, *Angew. Chem. Int. Ed.*, 2001, **40**, 2443.
7. J. J. Morris, B. C. Noll and K. W. Henderson, *Chem. Commun.*, 2007, 5191.
8. D. Maspoch, N. Domingo, D. Ruiz-Molina, K. Wurst, J.-M. Hernández, G. Vaughan, C. Rovira, F. Lloret, J. Tejada and J. Veciana, *Chem. Commun.*, 2005, 5035.